PROTECTION OF TRANSMISSION LINES AGAINST SWITCHING OVERVOLTAGES

A THESIS SUBMITTED TO
THE GRADUATE SCHOOL OF NATURAL AND APPLIED SCIENCES
OF
MIDDLE EAST TECHNICAL UNIVERSITY

BY

ERİNÇ EVREN ELMAS

IN PARTIAL FULFILLMENT OF THE REQUIREMENTS FOR
THE DEGREE OF MASTER OF SCIENCE

IN

ELECTRICAL AND ELECTRONICS ENGINEERING

DECEMBER 2004

Approval of the Graduate School of Natural And Applied Sciences

_____

Prof. Dr. Canan Özgen
Director

I certify that this thesis satisfies all the requirements as a thesis for the degree of Master of Science.

_____

Prof. Dr. İsmet ERKMEN
Chair of Electrical & Electronics Engineering Department

This is to certify that we have read this thesis and that in our opinion it is fully adequate, in scope and quality, as a thesis for the degree of Master of Science.

_____

Prof. Dr. Arif Ertaş
Supervisor

Examining Committee Members (first name belongs to the chairperson of the jury and the second name belongs to supervisor)

Prof. Dr. Nevzat Özay	(ODTÜ,EE)	_____
Prof. Dr. Arif Ertaş	(ODTÜ,EE)	_____
Prof. Dr. Ahmet Rumeli	(ODTÜ,EE)	_____
Prof. Dr. Mirzahan Hızal	(ODTÜ,EE)	_____
MS.Eng. Abdullah NADAR	(BİLTEN)	_____

I hereby declare that all information in this document has been obtained and presented in accordance with academic rules and ethical conduct. I also declare that, as required by these rules and conduct, I have fully cited and referenced all material and results that are not original to this work.

Name, Last name : Erinç Evren,Elmas

Signature:

ABSTRACT

PROTECTION OF TRANSMISSION LINES AGAINST SWITCHING OVERVOLTAGES

ELMAS, Erinç Evren

M.S., Department of Electrical and Electronics Engineering

Supervisor: Prof. Dr. Arif ERTAŞ

December 2004, 83 pages

Any switching action or lightning stroke on a transmission system causes excessive of voltage, which are propagated through the equipment. The withstand capability of the electrical equipment to these overvoltages is dependent on the rate of rise, peak value and the duration of these overvoltages and are especially critical to information technology (IT) equipment.

Whenever there is a probability of these overvoltages appearing across the electrical equipment, they should be limited to a safe value by the application surge arresters of the metal oxide type. However, surge arresters are expensive, an optimal location for these should be found so as to minimise the number of surge arresters used.

Key words: Switching overvoltage, High voltage (HV), Re-energization, Surge arrester, EMTP.

ÖZ

TAŞIMA HATLARININ ANAHTARLAMA AŞIRI GERİLİMLERE KARŞI KORUNMASI

ELMAS, Erinç Evren
Yüksek Lisans , Elektrik ve Elektronik Mühendisliği Bölümü
Tez Yöneticisi: Prof. Dr. Arif ERTAŞ
Aralık 2004, 83 sayfa

Bir iletim sisteminde, herhangi bir anahtarlama veya yıldırım darbesi, kullanılan elektriksel malzemelere doğru ilerleyen aşırı gerilime neden olur. Elektriksel malzemelerin aşırı gerilimlere dayanım kapasitesi, aşırı gerilimlerin yükselme oranına, tepe değerine ve süresine bağlı olup, bu aşırı gerilimlerin, özellikle de bilgi teknolojisi malzemeleri üzerindeki etkisi oldukça önemlidir.

Bir elektrik sisteminde, elektriksel malzemelere zarar verebilecek aşırı gerilim olasılığı varsa, bu aşırı gerilimler, metal oksit tipi parafudr uygulamalarıyla güvenli seviyede sınırlandırılmalıdır. Ayrıca, parafudrların pahalı olmasından dolayı, kullanılan parafudrların sayısını azaltacak en uygun yerler belirlenmelidir.

Anahtar Kelimeler: Anahtarlama Aşırı Gerilimleri, Yüksek Gerilim, Tekrar Enerjileme, Parafudr, EMTP

To My Family

ACKNOWLEDGEMENTS

I would like to express my sincere thanks to my supervisor, Prof. Dr. Arif ERTAŞ for his support during my studies at METU.

I owe special thanks to Prof. Dr. Nevzat ÖZAY for his guidance throughout my thesis.

I thankfully acknowledge the kind assistance of Mr. Osman Bülent TÖR.

Finally, my sincere thanks go to my family members whose support I felt throughout my studies.

TABLE OF CONTENTS

PLAGIARISM.....iii

ABSTRACT.....iv

ÖZ.....v

ACKNOWLEDGEMENTS.....vi

DEDICATION vii

TABLE OF CONTENTS.....vii

CHAPTER

1. INTRODUCTION.....1

2. ENERGIZATION ANALYSIS.....5

2.1 Introduction.....5

2.1.1 Definitions.....6

2.1.2 Classification of switching surges.....6

2.1.3 Energization of transmission lines.....8

2.2. Methodology.....8

2.2.1. Simulation of switching operations.....8

2.2.1. System design.....9

2.2.2. Scenarios.....9

2.3. Network modelling.....10

2.3.1. Transmission lines.……..…..10

2.3.2. Voltage source.....….....10

2.3.3. Circuit breaker.....…….....11

2.3.3.1 Statistical distribution of switching overvoltages.....12

2.4. Simulation results.…….....……...13

2.4.1. The effect of line length during energization…...…….....13

2.4.2. The effects of source inductance during energization…….23

2.5 Re-energization analysis….…….....…….....25

2.5.1 Nature of trapped charges...…….....26

2.5.2. Simulation results...…….....26

3. MEANS OF REDUCTION OF SWITCHING SURGES.....31

3.1. Introduction....…….....31

3.2. Resistor Energization…….....32

3.3. Application of Lightning arresters.....33

3.3.1 SiC Arresters……..……..…..…….....35

3.3.2 ZnO Arresters……..……..…..…….....39

4. OVERVOLTAGE PROTECTION BY SURGE ARRESTER.….....45

4.1. Introduction.....…….....45

4.2. Application of metal oxide (ZnO) surge arrester.....….....46

4.2.1 System modelled.…….....46

4.3. Re-energization simulations and utilization of surge arresters at different locations……..…….....46

4.3.1 Simulation of re-energization of Hopa-Enguri transmission line from Enguri side without arresters (case1)…….……..….46

4.3.2 Simulation of re-energization of Hopa-Enguri transmission line from Hopa side without arresters (case2)……..……49

4.3.3 Simulation with one arrester placed at Hopa (A comparison of re-energization from Enguri and re-energization from Hopa) ……..…….52

4.3.4 Simulation with one arrester placed at Enguri and a comparison of characteristics when the system is re-energized from Hopa and re-energized from Enguri……..…..…….…….58

4.3.5 Simulation with one arrester placed in the midst of Vardnili-Batum line ……...…….…..….62

4.3.6 Simulations with two arresters placed in the midst of Vardnili-Batum line Enguri ...…….…..….65

4.3.7 Simulation with arresters placed in the midst of Vardnili-Batum line and Hopa…..…….…..….68

4.3.8 Simulation with two arresters placed at Enguri and Hopa...….69

4.3.9 Simulation with two arresters placed at Enguri and Hopa when the line is re-energized from Hopa…..…...…….73

4.3.10 Simulation with three arresters placed Hopa, Enguri and at the 71,5th km of Vardnili-Batum line……..…….....…….75

4.4 Simulation results ……79

5. CONCLUSION…….....80

5.1. Introduction.....…….....80

5.2. Comparison of energization versus re-energization …….…….....80

REFERENCES.....82

LIST OF TABLES

2.1 Chief causes of high switching surges 7

2.2 Overvoltage variations of transmission lines due to lengths..... 23

4.1 Overvoltages when the system is energized from Hopa and re-energized from Enguri (no arrester is used) 47

4.2 Overvoltages when the system is energized from Hopa and re-energized from Hopa (no arrester is used) 52

4.3 Overvoltages when the system is energized from Hopa and re-energized from Enguri (arrester is used at Hopa)..... 54

4.4 Overvoltages when the system is energized from Enguri and re-energized from Hopa (arrester is used at Hopa)..... 57

4.5 Overvoltages when the system is energized from Hopa and re-energized from Enguri (arrester is used at Enguri) 60

4.6 Overvoltages when the system is energized from Enguri and re-energized from Hopa (arrester is used at Enguri)..... 62

4.7 Overvoltages when the system is energized from Hopa and re-energized from Enguri (arrester is used at mid point of Batum-Vardnili line) 64

4.8 Overvoltages when the system is energized from Hopa and re-energized from Enguri (arresters are used at mid point of Batum-Vardnili line and Enguri)..... 67

4.9 Overvoltages when the system is re-energized from Enguri (arresters are used at mid point of Batum-Vardnili line and Hopa) 69

4.10 Overvoltages when the system is energized from Hopa and re-energized from Enguri (arresters are used at Hopa and Enguri busses)..... 72

4.11 Overvoltages when arresters are placed at Hopa and Enguri 62

4.12 Overvoltages when the system is re-energized from Hopa (arresters are placed at Hopa, Enguri and mid point of Vardnili-Batum line) 79

LIST OF FIGURES

2.1 Schematic diagram of the analyzed system 5

2.2 The steady state voltage magnitudes of three phases to ground at the terminals of the source 11

2.3 Representation of switches in EMTP 11

2.4 Basic circuit: representation of energization of a line 12

2.5 Three phase waveforms at the end of the line of 50 km length, energized by 126 kV 13

2.6 Distribution of overvoltages in pu. for 50 km. length line model 14

2.7 Sending end voltage waveforms of phase A of a 50 km length line, energized by 126 kV 15

2.8 Three phase wave forms at the end of the line of a length 100 km, energized by 126 kV 15

2.9 Sending end and receiving end voltage waveforms of phase A of a 100 km length line, energized by 126 kV 16

2.10 Distribution of overvoltages in pu for the 100 km length line model 16

2.11 Three phase waveforms at the end of the line of a length 150 km, energized by 126 kV 17

2.12 Sending end and receiving end voltage waveforms of phase A of a 150 km length line, energized by 126 kV 17

2.13 Distribution of overvoltages in pu for the 150 km length line model 18
2.14 Three phase waveforms at the end of the line of a length 200 km, energized by 126 kV 18
2.15 Sending end and receiving end voltage waveforms of phase A of a 200 km length line, energized by 126 kV 19
2.16 Distribution of overvoltages in pu for the 200 km length line model 19
2.17 Three phase waveforms at the end of the line of a length 250 km, energized by 126 kV 20
2.18 Sending end and receiving end voltage waveforms of phase A of a 250 km length line, energized by 126 kV 20
2.19 Distribution of overvoltages in pu for the 250 km length line model 21
2.20 Comparison of receiving end voltages of different lengths: 50, 100, 150 km ... 21
2.21 Comparison of receiving end voltages of different lengths: 150, 200, 250 km . 22
2.22 Comparison of receiving end voltages of different lengths: 50, 200 km 22
2.23 Comparison of different source inductances: 95.3, 47.65 mH 24
2.24 Comparison of frequency of occurrence of overvoltages for different source inductances 24
2.25 Comparison of different source inductances: 95.3, 142.95 mH 25
2.26 Histogram of the distribution of peak overvoltages among all output nodes of the 50 km line (A comparison of energization/ re-energization overvoltages) 26
2.27 Re-energization overvoltages of 50 km line 27
2.28 Re-energization overvoltages at the receiving end of 100 km line 27
2.29 Frequency of occurrence of re-energization overvolyages in pu values in phase B at the receiving end of 100 km line 27

2.30 Comparison of re-energization overvoltages of 50 km and 100 km lines 28
2.31 Re-energization overvoltages at the receiving end of 150 km line 28
2.32 Histogram of the distribution of peak overvoltages among all output nodes of the 150 km line 28
2.33 Re-energization overvoltages at the receiving end of 200 km line 29
2.34 Re-energization overvoltages at the receiving end of 250 km line 29
2.35 A comparison of frequency of occurrence of re-energization overvoltages at the receiving end of 200 and 250 km lines 29
3.1 The operation principle of closing resistors 32
3.2 Nonlinear characteristic of a 220 kV silicon-carbide surge arrester 37
3.3 Arrester sparkover voltage time characteristic for wave fronts with linear rise 38
3.4 Arrester gap characteristic 39
3.5 Voltage-current characteristic of a 1200 kV gapless metal-oxide surge arrester. 40
3.6 Two-section surge arrester model for fast front surges 42
3.7 Alternative surge arrester model 43
3.8 Metal-oxide surge arrester with shunt spark gap 43
4.1 Transmission line configuration (no arrester is used) 46
4.2 Histogram of voltage distribution for the maximum of the peaks at all output nodes. (No arrester is used 47
4.3 Receiving end voltage of line at Hopa (no arrester is used) 47
4.4 Histogram of voltage distribution for the maximum of the peaks at Hopa bus phase C (No arrester is used) 46
4.5 Receiving end voltage of line at Enguri (no arrester is used) 48

4.6 Histogram of voltage distribution for the maximum of the peaks at Enguri. (No arrester is used..... 49
4.7 Transmission line configuration (no arrester is used)..... 49
4.8 Histogram of voltage distribution for the maximum of the peaks at all output nodes. (No arrester is used) 50
4.9 Histogram of voltage distribution for the maximum of the peaks at the beginning of Hopa-Border line. (No arrester is used)..... 50
4.10 Receiving end voltage of line at Enguri (no arrester is used) 51
4.11 Histogram of voltage distribution for the maximum of the peaks Enguri phase C (no arrester is used) 51
4.12 Receiving end voltage of line at Enguri (no arrester is used) 510 Receiving end voltage of line at Enguri (no arrester is used) 51
4.13 Location of the first surge arrester installed at..... 52
4.14 Histogram of voltage distribution for the maximum of the peaks at all output nodes when the system energized from Enguri and one arrester is used at Hopa 53
4.15 Receiving end voltage of line at Hopa when an arrester is used at Hopa 53
4.16 Power characteristic of surge arrester at Hopa (phase A)..... 54
4.17 Energy absorption characteristic of surge arrester at Hopa when an arrester is used at Hopa (of Phase A)..... 54
4.18 Sending end voltage of line at Hopa when an arrester is used at Hopa and line is re-energized from Hopa 55
4.19 Histogram of voltage distribution for the maximum of the peaks of Hopa bus phase C when the system re-energized from Hopa and one arrester is used at Hopa 55

4.20 Receiving end voltage of line at Enguri when an arrester is used at Hopa and line is re-energized from Hopa 56
4.21 Histogram of voltage distribution for the maximum of the peaks of Enguri phase C when the system re-energized from Hopa and one arrester is used at Hopa 56
4. 22 Power characteristic of surge arrester at Hopa when an arrester is used at Hopa (of Phase C) 57
4. 23 Energy absorption characteristic of surge arrester at Hopa when an arrester is used at Hopa (of Phase C) 57
4.24 Location of the surge arrester installed at Enguri 58
4.25 Histogram of voltage distribution for the maximum of the peaks of overall nodes when the system re-energized from Enguri and one arrester is used at Enguri 58
4. 26 Power characteristic of surge arrester at Hopa when an arrester is used at Enguri (Phase A) 59
4. 27 Energy absorption characteristic of surge arrester at Hopa when an arrester is used at Enguri 59
4. 28 Network configuration of the system with surge arrester at Enguri re-energization from Hopa Bus 60
4. 29 Histogram of voltage distribution for the maximum of the peaks of overall nodes when the system re-energized from Hopa and one arrester is used at Enguri . 60
4. 30 Histogram of voltage distribution for the maximum of the peaks at Hopa Bus when the system re-energized from Hopa and one arrester is used at Enguri 61
4. 31 Power characteristic of surge arrester at Enguri 61

4. 32 Energy characteristic of surge arrester at Enguri 61

4. 33 Location of the surge arrester installed at 71.5 km further than Batum..... 62

4. 34 Receiving end voltage of line at Hopa when an arrester is used at 71.5 km further than Batum 63

4. 35 Histogram of voltage distribution for the maximum of the peaks at Hopa Bus phase A when the system re-energized from Hopa and one arrester is used at mid-point of Batum-Vardnili line 63

4. 36 Power characteristic of surge arrester at Hopa when an arrester is used at 71.5 km further than Batum 63

4. 37 Energy absorption characteristic of surge arrester at Hopa when an arrester is used at 71.5 km further than Batum 64

4. 38 Arresters located at Enguri and at 71.5 km further than Batum..... 65

4. 39 Voltage at Hopa open end when arresters are located at Enguri and at 71.5 km further than Batum 65

4. 40 Histogram of overvoltage distribution at Hopa Bus (Phase A)..... 65

4. 41 Power characteristic of surge arrester in the middle of Vardnili-Batum line when arresters are located at Enguri and at 71.5 km further than Batum 66

4. 42 Energy characteristic of surge arrester in the middle of Vardnili-Batum line when arresters are located at Enguri and at 71.5 km further than Batum 66

4. 43 Power characteristic of surge arrester at Enguri when arresters are located at Enguri and at 71.5 km further than Batum..... 67

4. 44 Energy characteristic of surge arrester at Enguri when arresters are located at Enguri and at 71.5 km further than Batum..... 67

4. 45 Arresters located at Hopa and at 71.5 km further than Batum..... 68

4. 46 Power characteristic at Hopa when arresters are located at Hopa and at 71.5 km further than Batum 68

4. 47 Energy characteristic of surge arrester at Hopa 68

4. 48 Power characteristic of surge arrester at mid point when arresters are placed at Hopa and mid point of Vardnili 69

4. 49 Energy characteristic of surge arrester at mid point when arresters are placed at Hopa and mid point of Vardnili 69

4. 50 Arresters located at Hopa and at Enguri 70

4. 51 Histogram of overvoltage distribution at all output nodes..... 70

4. 52 Power characteristics of surge arrester located at Enguri when arresters are placed at Hopa and at Enguri 70

4.53 Energy characteristics of surge arrester located at Enguri when arresters are placed at Hopa and at Enguri 71

4. 54 Power characteristics of surge arrester located at Enguri when arresters are placed at Hopa and at Enguri 71

4. 55 Energy characteristics of surge arrester located at Enguri when arresters are placed at Hopa and at Enguri 72

4. 56 Location of the surge arrester installed at Hopa and Enguri..... 73

4. 57 Power characteristics of the surge arrester placed at Hopa..... 73

4. 58 Energy characteristics of the surge arrester placed at Hopa 73

4. 59 Power characteristics of the surge arrester placed at Enguri..... 74

4. 60 Energy characteristics of the surge arrester placed at Enguri 74

4. 61 Transmission line configuration (with 3 arresters) 75

4. 62 Receiving end voltage of line at Hopa when 3 arresters are used..... 75

4. 63 Histogram of overvoltage distribution at Hopa Bus (Phase C)..... 75

4. 64 Power characteristic of surge arrester at Hopa..... 76

4. 65 Energy characteristic of surge arrester at Hopa 76

4. 66 Voltage characteristics at Enguri bus 76

4. 67 Histogram of overvoltage distribution at Enguri Bus (Phase A) 77

4. 68 Power characteristic of surge arrester at Enguri 77

4. 69 Energy characteristic of surge arrester at Enguri 77

4. 70 Voltage characteristics at mid point of Vardnili-Batum 77

4. 71 Voltage distribution at Enguri (Phase A) 78

4. 72 Power characteristic of surge arrester at mid point 78

4. 73 Energy characteristic of surge arrester at mid point..... 78

CHAPTER 1

INTRODUCTION

In the normal operation of power systems, unavoidable disturbances may happen due to sag, swell, noise, and overvoltage surges. Sag, swell and noise can upset electronic appliances, but are unlikely to cause permanent damage. Overvoltage surges, however, are damaging in nature and result in more frustrations and even fire in rare cases. An overvoltage disturbance occurs in power systems when the network experiences a change of state. Lightning and switching action are the two reasons of creating a surge. The problem of switching surges had become a problem acquiring equal or greater care during study with respect to lightning for the selection of insulation and protection levels. [1]

Switching operations in power systems can produce transient overvoltages whose maximum peaks depend on several factors, for instance the network on the source side of the circuit breaker, or the trapped charge in reclosing operations of transmission lines. [2] The calculation of switching overvoltages is fundamental for the insulation design of many power components. However equipment insulation design is not usually based on the highest overvoltage since this particular event is a low probability of occurrence, and the design would not be economical. Besides in many cases, it can be very difficult to determine the combination of parameters that will produce the highest overvoltage.

When a circuit breaker is closed applying a voltage to a line, during switching operations, a voltage wave accompanied by a current wave starts to travel along the line. If the receiving end of the line is open circuited, the magnitude of the

voltage will double at the receiving end. The reflected wave toward the sending end will cause new reflections. These reflections may cause the receiving end voltage to increase to values above 2.0 pu during transient period.

If the re-energization operation takes place after a fault, the magnitude of traveling voltage wave will increase due to the trapped voltage on the line. The overvoltage values at the open end of the line may reach to 4.0 pu. the insulation level of the transmission line is determined due to these transients during overvoltages. It is very important to analyze the overvoltage values and take the precautions at the design stage of the transmission line.

The insulation design of power equipment is based on the concepts of stress and strength. The probability distribution of switching overvoltages is to be compared to equipment insulation.

A reliable way of protecting electrical equipment against excessive voltage resulting, for instance, from switching operations, short circuits, resonance effects and atmospheric discharge is to use a surge protective device (a surge arrester or surge diverter).

What these devices do is neither to suppress nor arrest a surge but simply divert it to ground, where it can do no harm. The modern surge protective devices consist of a metal oxide varistor (mainly ZnO) being embedded in a ceramic insulator. As soon as excess voltage is given, the arrester's non-linear resistance decreases so much, that the excess voltage is restricted. For this reason the arrester's grounding must be as low as possible. The secondary current, still flowing under the influence of the operating voltage, is also suppressed by the resistance, which is rapidly increasing again. At a given operating voltage, surge arresters with metal oxide varistors exhibit a very high resistance and therefore, have got only insignificant leakage current. Lightning arresters have been successively used for station protection.

The ideal solution for lightning protection is to install the lightning arresters in the immediate neighborhood of each equipment to be protected, which is unfortunately costly. Therefore, the aim is to provide overvoltage protection to all appliances in a system with fewer lightning protective devices.

The energy to be dissipated in the case of switching surges is very much higher than that of a lightning surge recent times, lightning (surge) arresters could not been used for the reduction of surge magnitudes. Surge arresters with very high energy absorption capabilities are now available.

The research aims to investigate energization and re-energization surges expected to be generated on a 154 kV line. A study was then undertaken to see how surge arresters could be used to protect a given system against unacceptable overvoltage levels appearing in the system. Finally the cases are repeated for a real system on a new interconnection between Turkey and Georgia.

The thesis is divided into 5 chapters. Chapter 2 reviews the analysis of overvoltages appearing in the system due to energization and re-energizaiton. Chapter 3 outlines the means of reduction of switching surges followed by the research findings on the application of surge arrester for overvoltage protection on a real system in Chapter 4.

The studies are carried out through computer simulations, using ATPDraw. This is a graphical, mouse-driven preprocessor to the Alternative Transient Program (ATP) version of Electro-Magnetic Transient Program (EMTP) on the MS-Windows platform. The program is written in Borland Delphi 2.0. and runs under Windows 9x/NT/2000/XP. In ATPDraw the user can construct an electric circuit using the mouse and selecting components from menus, and then ATPDraw generates the ATP input file in the appropriate format based on “what you see is what you get”. ATP is a general-purpose computer program for simulating high-speed transient effects in electrical power systems. The program features an extremely wide variety of modeling capabilities encompassing electromagnetic

and electromechanical oscillations ranging in duration from microseconds to seconds. [3]

Finally, conclusions and recommendations of the research are given in Chapter 5.

CHAPTER 2

ENERGIZATION ANALYSIS

2.1 INTRODUCTION

In this chapter, overvoltage due to energization is analysed. First, the methodology of how the analysis is carried out is presented in Section 2.2. The modelling of the considered system components is discussed in Section 2.3, followed by the simulation results in Section 2.4.

In a simple circuit as shown in Fig. 2.1, if the switch operates in an ideal manner, the theoretical value of the overvoltage magnitude does not exceed twice the system voltage. An ideal operation could be defined as closing the switch by a single make action or opening the switch by a single break action at current zero. However, switching operations in practical systems deviate from this theoretical value because of the interaction of many variables possessed either by the system, or the switch, or by a combination of both. These include source impedances, transformer excitation characteristics, line impedance and termination characteristics, Ferranti effect, the presence or absence of shunt reactors and series capacitors during closing or opening operations.

Figure 2.1 Schematic diagram of the analysed system

2.1.1 Definitions

Usually the term switching surge is used to refer to voltage transients and it can be defined with respect to amplitude and waveform only by reference to a given point of the system, although in practice, data on overvoltage magnitudes are assumed to be applicable to any point of the system, or part of the system concerned. The amplitude of a switching surge voltage transient is expressed in terms of its peak voltage and is usually referred to as an overvoltage factor, k, which is the ratio of the peak voltage of the transient to a reference voltage. It is customary to take the reference voltage as the peak phase-to-ground voltage $(2/3)^{1/2}E$, where E is the nominal system r.m.s. line voltage.

The waveform of the switching surge, which can take so many forms, has been neglected in many of the analysis, and the most pessimistic case has been assumed to occur when applied to system insulation.

The wavefront duration time, T, of the switching surge voltage is the time from its beginning to the crest. However, for waves having a slow initial rate of rise followed by a comparatively rapid rate of rise, and then a final slow levelling-off to the crest, it is customary to ignore the slower rates of rise and to consider the effective front which is defined as "1.67 times the time interval between the instants when the voltage is 30 and 90 percent of the peak value".

2.1.2 Classification of Switching Surges

The name switching surge usually covers all the transient voltages which are produced by one complete operation, either closing or opening of a switch. Analysis of the transient phenomena during a switching operation makes it desirable to recognise three distinct phases of overvoltages [4]:

1. A surge period, in which travelling wave effects predominate and in which system elements are represented by their distributed constants. It starts with the closing of the first breaker pole and ends with the vanishing of travelling

wave effects, lasting around five or six round trips of the travelling wave after the last breaker pole has been closed.

2. A dynamic period, which is the time between the surge period and the steady-state condition, generally continuing for several cycles. It is characterised by voltage variation contained in an envelope which varies aperiodically with time.

3. A steady-state period in which, amplitudes and waveform of the voltage is periodic irrespective of harmonic content.

In this thesis, work is centered on the first period, i.e., the surge period, during which the highest overvoltages are produced and therefore, it is the most important factor in the determination of the insulation levels of the systems. In table 2.1 the chief causes of high surge period overvoltages in EHV are listed. These are not necessarily independent of one another, and are influenced by the circuit configuration involved on both sides of the switch.

Table 2.1. Chief Causes of High Switching Surges

1. Energisation of open ended lines
2. High-speed reclosure
3. Presrikes and restrikes
4. Current chopping
5. Disconnecting faulted lines
6. Load rejection
7. Single phase switching in three phase systems

In the majority of EHV systems, the predominant switching overvoltages are those arising from the energization of unloaded lines with or without residual voltages on these lines if re-strike free breakers are used. Because of electrical coupling between phases and sequential closing among poles of the circuit breaker, the maximum magnitude of switching surges on a transmission line that is being energised can be as severe as from re-striking, and reclosing on a line with trapped charge greatly increases the overvoltage magnitudes beyond normal energization.

If no means are employed to reduce the overvoltage magnitudes caused by line energisation and reclosing, then other switching operations need not be considered with regard to insulation requirements since the anticipated switching surges are relatively low.

2.1.3 Energization of Transmission Lines

The magnitude and waveform of a switching surge are influenced by the circuit configuration involved on each side of the switch, namely the source and the line sides. However, in general the source is not a localized generation which can be represented by its transient reactance, but terminating at the bus may be other transmission lines originated at some remote point in the system in which in turn could be fed from other generating points.

One variable in the transient analysis of a transmission line which is closely linked to the source representation is the observation time chosen for the study. As the transit times to the distant points of such complex networks may exceed the observation period chosen, they would have no direct relevance to the study. Therefore it may not be required to represent the entire source network configuration. A careful analysis of the system is necessary to determine which parts of the system could be omitted.

2.2 METHODOLOGY

2.2.1 Simulation of Switching Operations

This section describes the system employed in the study on the investigation of overvoltage levels appearing in the system due to switching transients.

Any switching operation is either an opening of a circuit in which the current through the switch is interrupted, or closing of a circuit during which the voltage

across the switch is cancelled. Using the superposition theorem, these boundary conditions can be satisfied with the ideal current and voltage sources. Thus, during the case of opening of a circuit, if an equal but opposite in sign, current is injected through the contacts of switch; this would cancel the current, thereby simulating the opening of the switch. A similar argument can be applied to closing of a circuit. The voltage across the switch is to be nullified, and this is achieved by superimposing an equal but opposite in polarity voltage across the contacts.

In both cases, the resultant voltages and currents in any part of the circuit would be given by those due to the cancellation voltages and currents superimposed to those which would exist if the switches were not operated.

2.2.2 System design

A number of factors are involved in transmission systems that may give rise to an unacceptable level of overvoltage when the line is energized. These include the length of feeders, source inductance etc. Therefore, a system is built to analyse the above-mentioned effects.

The system is designed broadly to examine the insulation level in case of switching operations, using the parameters of 154 kV transmission line.

2.2.3 Scenarios

The study is mainly divided into two different scenarios:

1. System with different length of line.
2. System where the value of inductance of the source is changed.

In scenario 1, the length of line is varied from 50 to 250 km. With all other parameters are kept constant. The aim of this scenario is to investigate the effect of length of lines on overvoltage appearing at the line ends.

In scenario 2, source inductance is changed from 95.3 mH to 47.65 and 190.6 mH. The goal is to see the effect of source inductance, which depends on the source short-circuit MVA, on overvoltages generated in the system.

2.3 NETWORK MODELLING

When a disturbance occurs in a power system, travelling waves are initiated. Travelling waves of current and voltage propagate along the conductors. On reaching a discontinuity, such as open circuit, or short circuit or at a point in the system where the characteristic impedance changes, some part of the wave is let through and the other is reflected back by a reflection coefficient, which depends on the value of the load impedance different from the characteristic impedance of the line conductor. This oscillatory nature of transient voltage waves may cause a voltage built up in the system, which is unacceptable. Therefore simulation of the transient phenomena in power systems very often requires detailed modelling of just a small part of the system to be studied.

2.3.1 Transmission Lines

The most accurate models of the power transmission lines for transient calculations are those that take into account the distributed nature of parameters. Therefore, the distributed parameter line model is used in simulations for the considered lines in order to obtain high degree of accuracy. The distributed parameters of the lines considered are calculated by utilising "LINE CONSTANTS" supporting routine of ATP computer simulation program with "JMARTI" output request [6]. With this model the frequency dependence of the line parameters are taken into account.

2.3.2 Voltage source

The voltage source representing the generator units are modelled as sinusoidal sources with 50 Hz frequency [6]. The magnitude of the source is selected such

that the steady state voltage magnitude at transformer primary terminals is 154 kV (line to line rms). The three phase voltage waveforms at the sending end are shown in Figure 2.2.

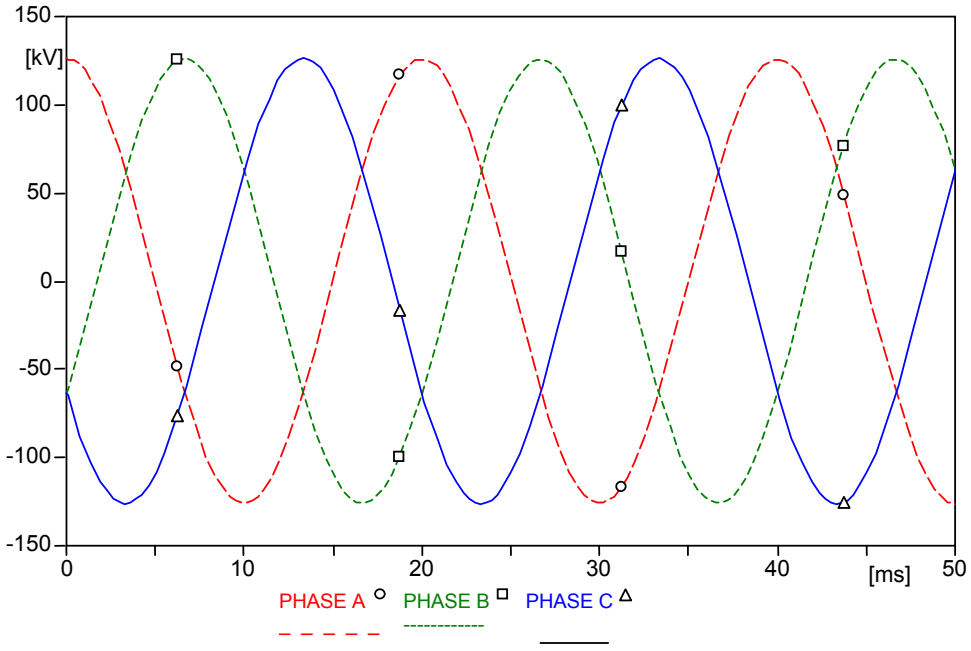

Figure 2.2 The steady state voltage magnitudes of three phases to ground at the terminals of the source

2.3.3 Circuit breaker

Circuit breakers are modelled at each end of the line in order to simulate switching actions. Any switching operation in a power system can potentially produce transients. All these switching devices are represented as ideal switches in the EMTP, with zero current ($R=\infty$) in the open position and zero voltage ($R=0$) in the closed position. If the switch between nodes k and m is open, then both nodes are represented in the system of nodal equations, whereas for the closed switch, both k and m becomes one node.

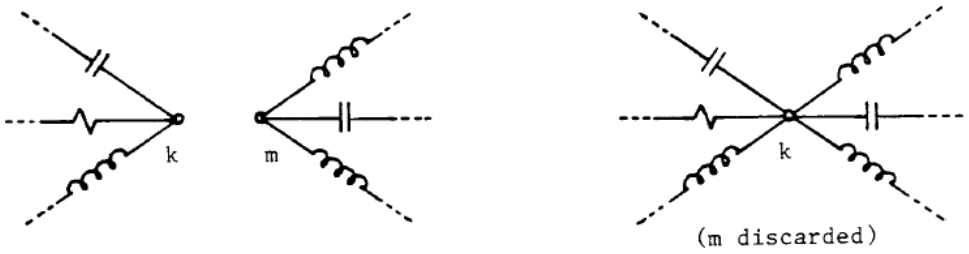

Figure 2.3 Representation of switches in EMTP

Types of switches used in this study are measuring switches, statistical switches and disconnecting switches which are all time-controlled switches.

2.3.3.1 Statistical Distribution of Switching Overvoltages

There is a time span between the first and last pole to close when a circuit breaker receives a closing signal. Travelling waves are initiated when a line is energized with one end open. They are reflected at the open end with the doubling effect, and transient overvoltages of 2 p.u. at the receiving end are therefore to be expected. In reality they may be higher due to some reasons. The closure of the first pole induces some voltage on the other two poles, which affects the maximum overvoltage value on the line. From this point of view we can say that the switching overvoltages have statistical nature, and it is necessary to calculate the overvoltages with statistical methods.

The closing time T_{close} for each "STATISTICS" switch is randomly varied according to either a Gaussian (normal) distribution or a uniform distribution. In addition to switch-closing time variation caused by each switch's own distribution, there is an added random delay which is the same for all switches.

Statistical methods are also necessary because the chance of obtaining the maximum overvoltage is very small, and therefore one need not take into account these values in the design of insulation levels. [2]

2.4 SIMULATION RESULTS

The result of energization studies of a dead line is mainly presented in this section. This section also presents the effects of line length and source inductance on switching transients. The effect of different scenarios on overvoltages at all line nodes is traced by investigating the voltage waveforms in the time domain.
Parameters effecting voltage values on the transmission line during energization can be expressed for this study as; length of the line and inductance of the source.

2.4.1 The effect of line length during energization

For the system modelled, with the overhead lines skin effect is taken into account and the lines are supposed to be transposed. JMarti model is used which is a frequency dependent one with constant transposition matrix. For each case to simulate energization a statistical switch is used and to obtain the frequency of occurrence versus overvoltages graph 100 switching is performed, which is sufficient to get an overall view of the overvoltage distribution.

To start with we will study effects of line length: the length of the line is examined for 50,100,150,200,250 km. As the length of the line is increased the total energy stored on the line is increased.

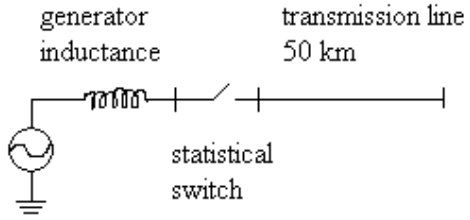

Figure 2.4 Basic circuit: representation of energization of a line

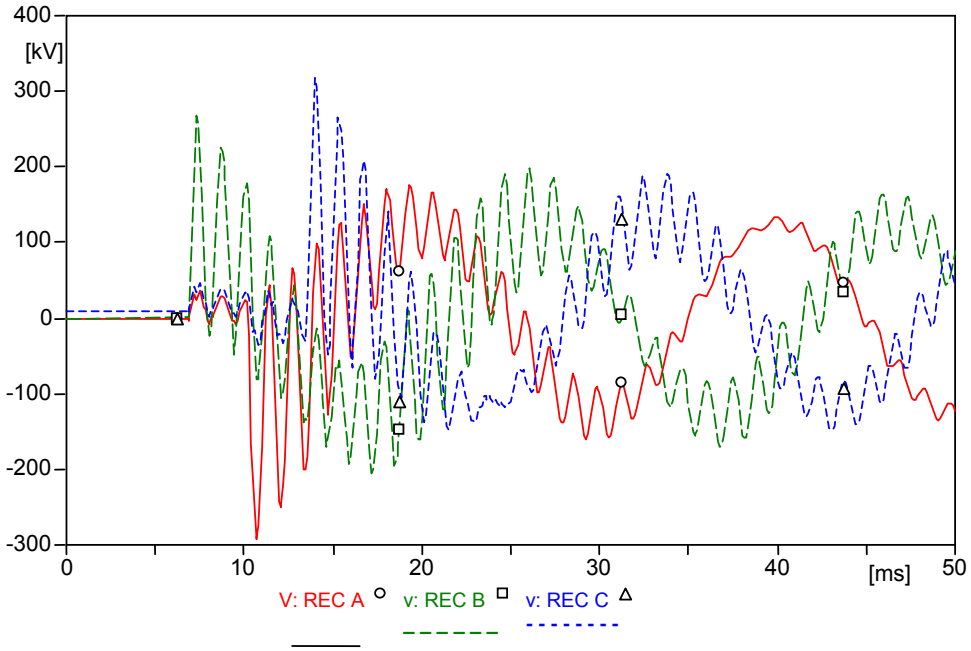

Figure 2.5 Three phase waveforms at the end of line of a length 50 km, energized by 126 kV

As seen from Figure 2.5, for the simulation for 50 km line energization overvoltage values are in sequences for phase A, B and C; 296 kV, 289 kV and 315 kV at the open end of the line meanwhile the source voltage is 126 kV. The following is a distribution of peak overvoltages among all output nodes for this case.

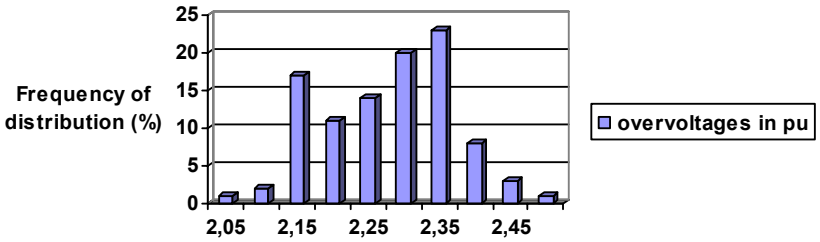

Figure 2.6 Distribution of overvoltages in pu for the 50 km length line model

The following is a comparison of sending and receiving end voltages within phase-A. 291 kV is observed for receiving end while 223 kV is recorded for sending end.

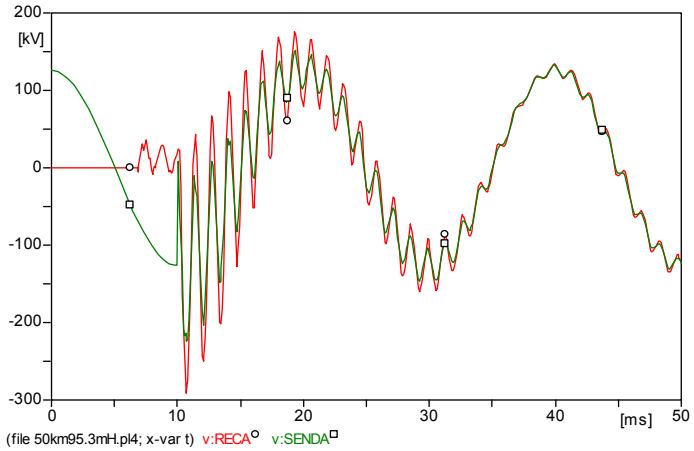

Figure 2.7 Sending end and receiving end voltage waveforms of phase A of a 50 km length line, energized by 126 kV

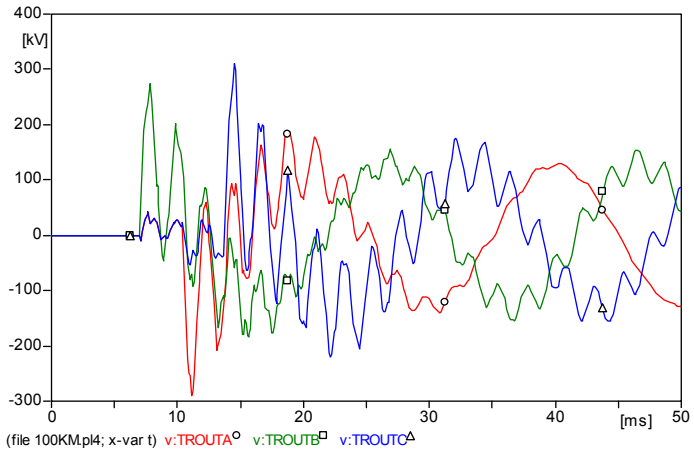

Figure 2.8 Three phase waveforms at the end of line of a length 100 km, energized by 126 kV

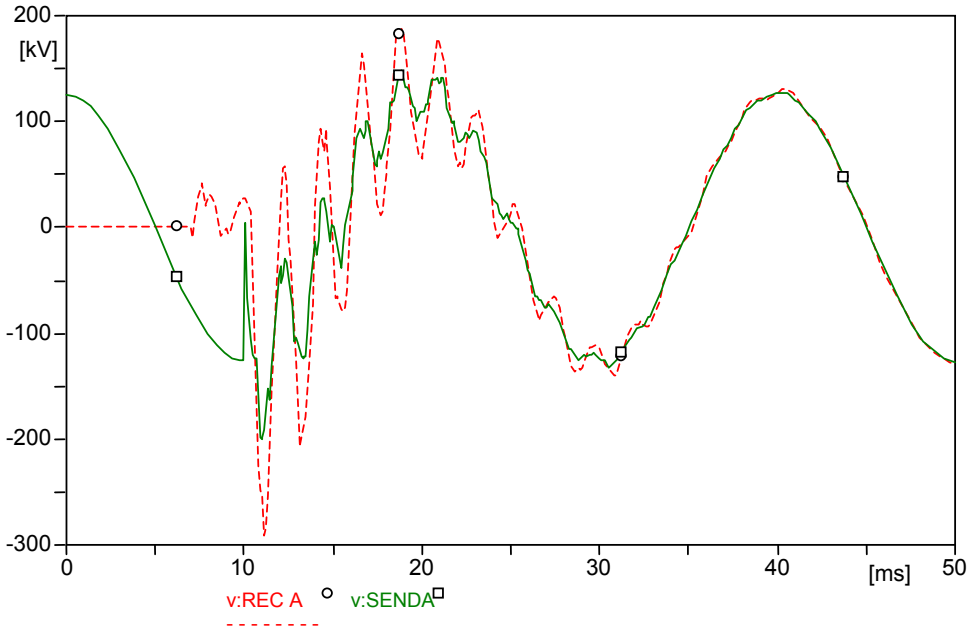

Figure 2.9 Sending end and receiving end voltage waveforms of phase A of a 100 km length line, energized by 126 kV.

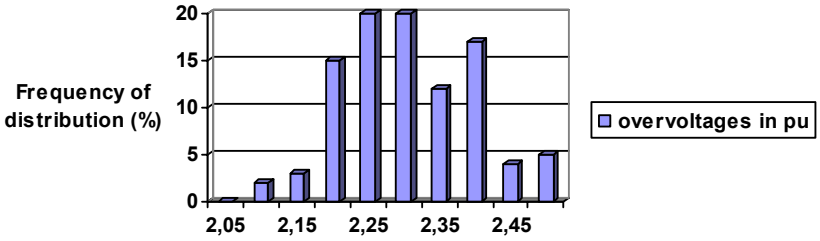

Figure 2.10 Distribution of overvoltages in pu for the 100 km length line model

As observed from the figures the overvoltage magnitudes at the receiving end of a line increase with the line length. However, for a three phase system, this increase is not a uniform one if a single case is analysed because the responses of systems with different line lengths are sensitive to the timing of the individual pole closure due to the variation of the natural frequency of the system with the line length. Because of that a statistical analysis is done to view effects of line length.

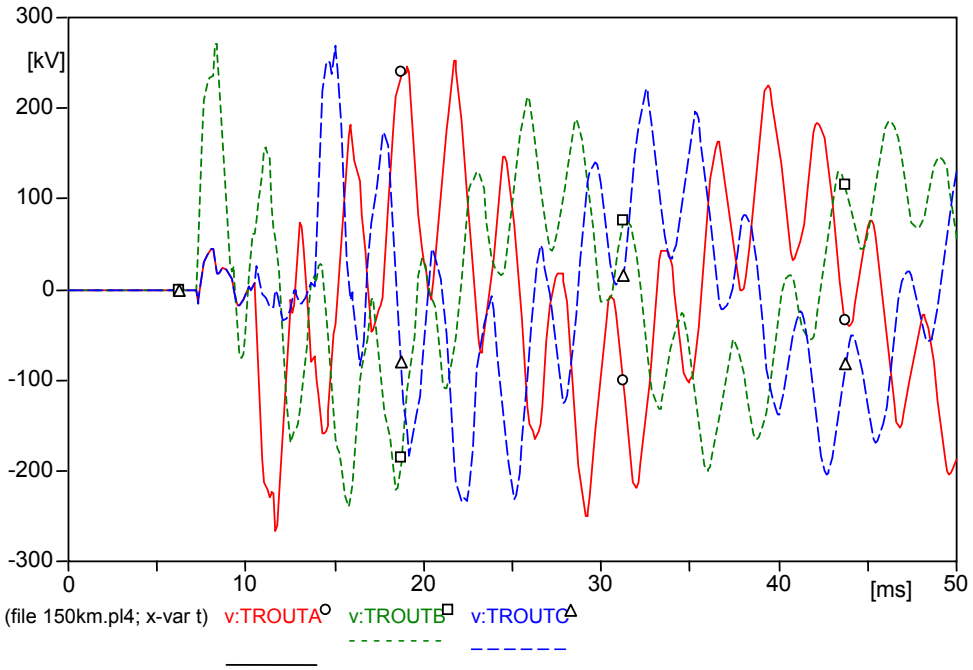

Figure 2.11 Three phase waveforms at the end of line of a length 150 km, energized by 126 kV

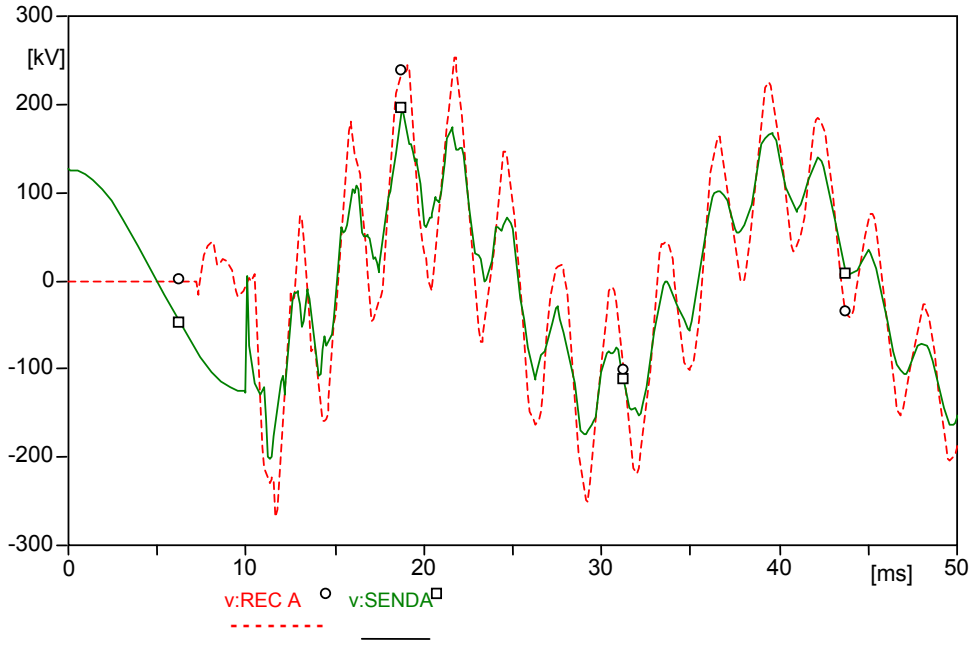

Figure 2.12 Sending end and receiving end voltage waveforms of phase A of a 150 km length line, energized by 126 kV

The following is the overvoltage distribution among all nodes for the case.

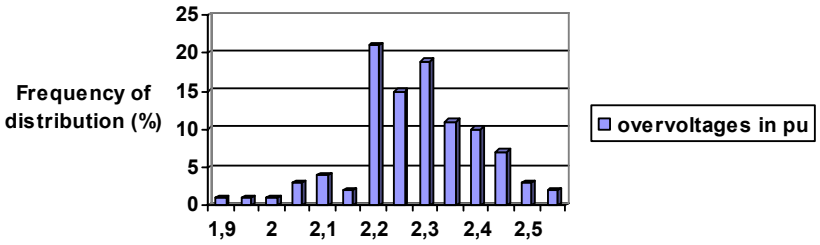

Figure 2.13 Distribution of overvoltages in pu for the 150 km length line model

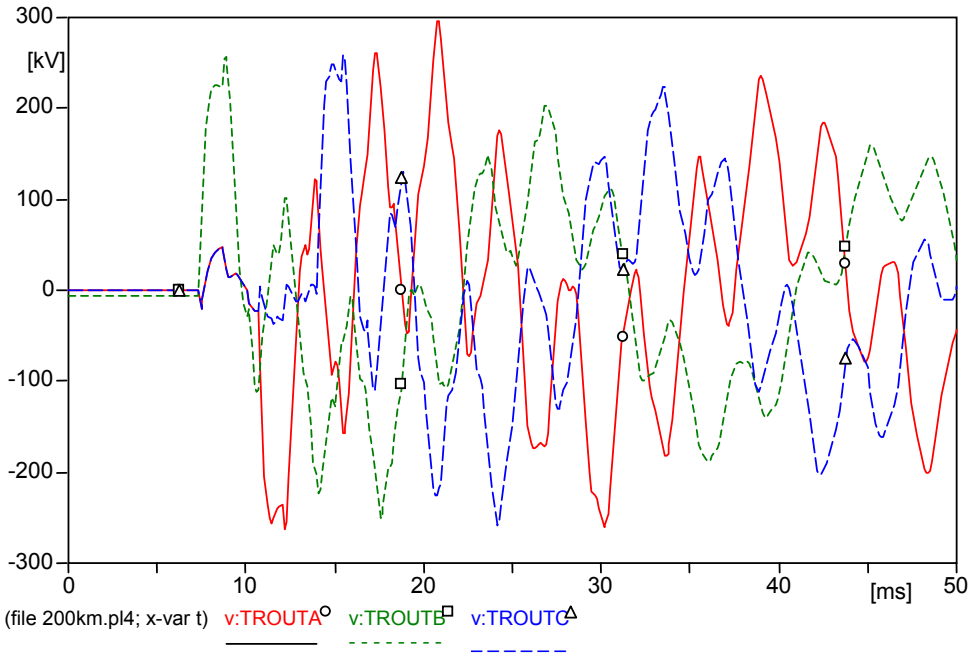

Figure 2.14 Three phase waveforms at the end of line of a length 200 km, energized by 126 kV

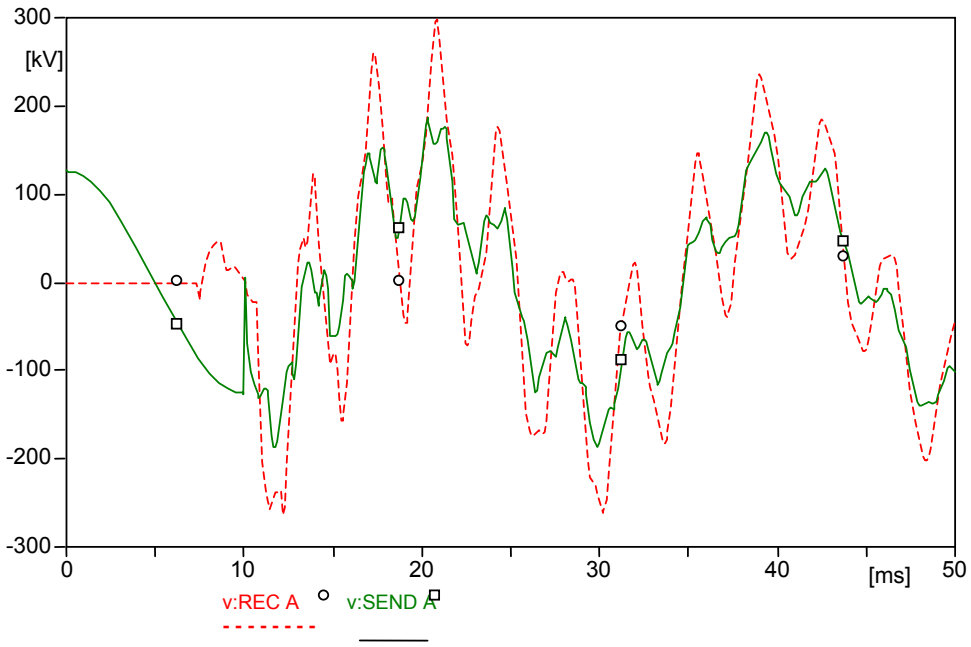

Figure 2.15 Sending end and receiving end voltage waveforms of phase A of a 200 km length line, energized by 126 kV

The following histogram is drawn for distribution of overvoltages overall nodes.

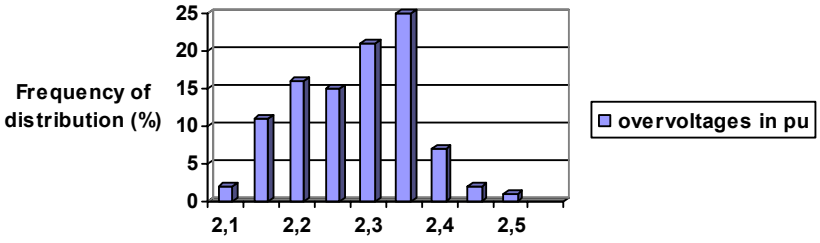

Figure 2.16 Distribution of overvoltages in pu for the 200 km length line model

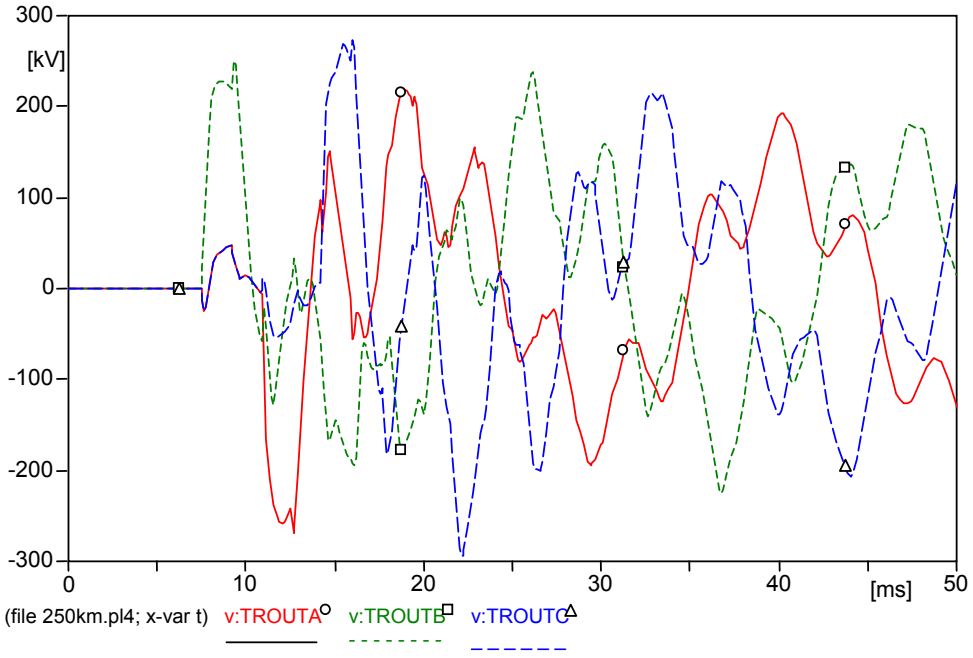

Figure 2.17 Three phase waveforms at the end of line of a length 250 km, energized by 126 kV

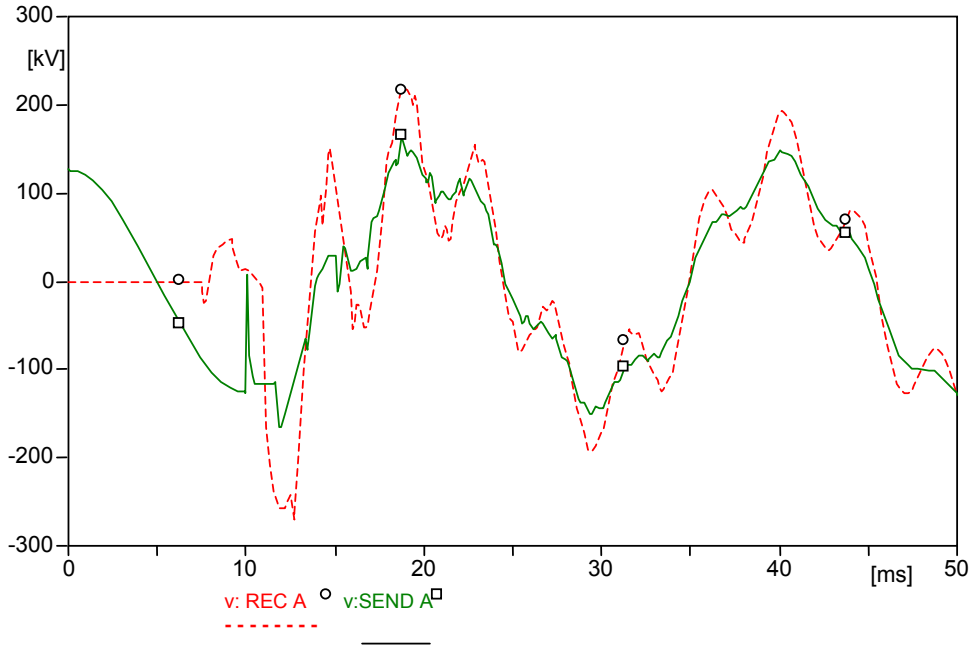

Figure 2.18 Sending end and receiving end voltage waveforms of phase A of a 250 km length line, energized by 126 kV

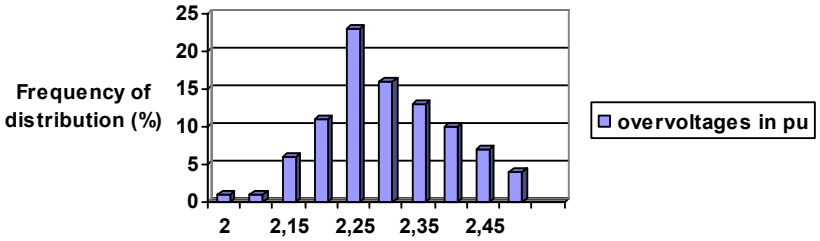

Figure 2.19 Distribution of overvoltages in pu for the 250 km length line model

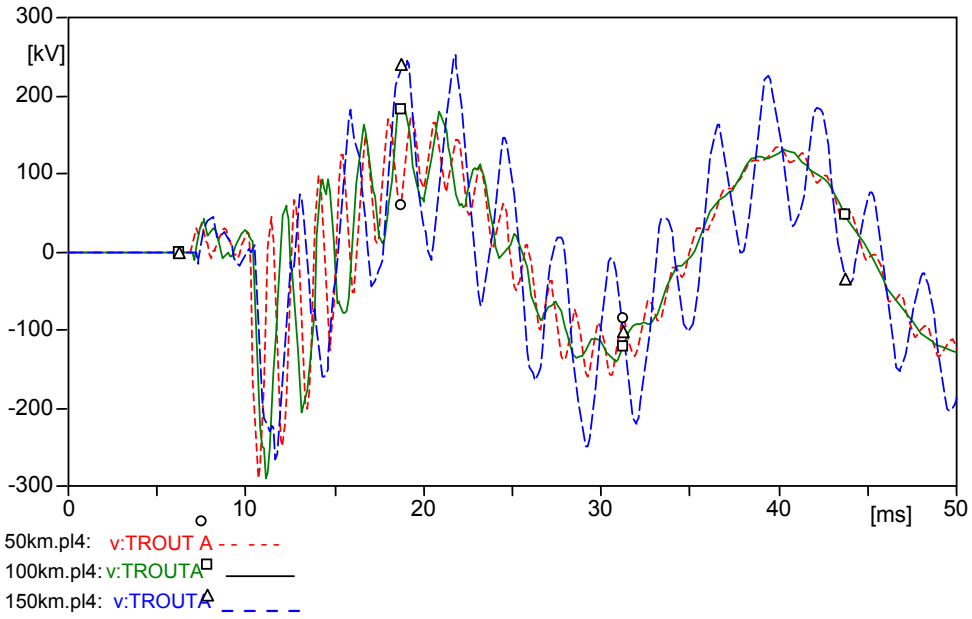

Figure 2.20 Comparison of receiving end voltages of lines of different lengths: 50,100,150 km

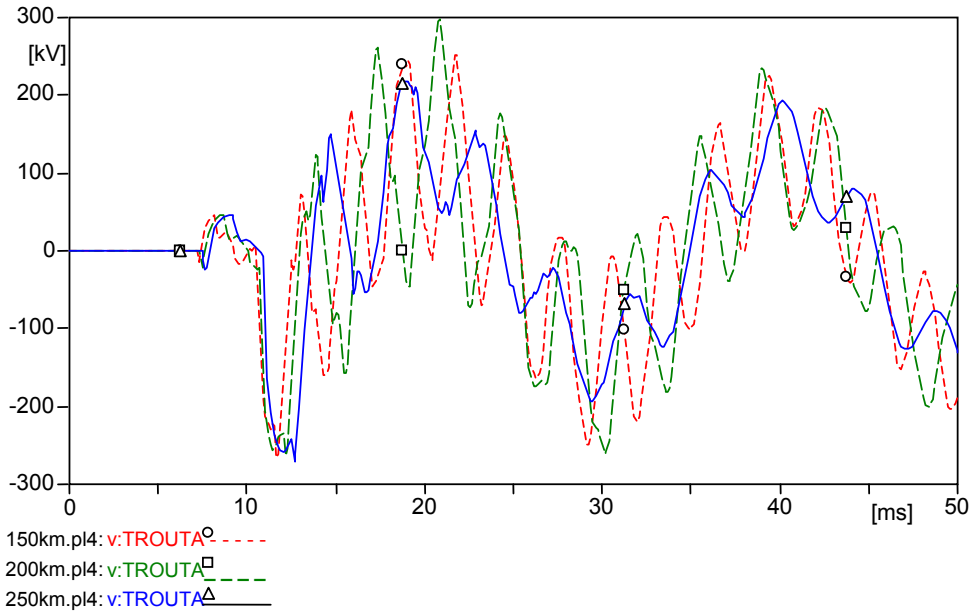

Figure 2.21 Comparison of receiving end voltages of lines of different lengths: 150,200,250 km

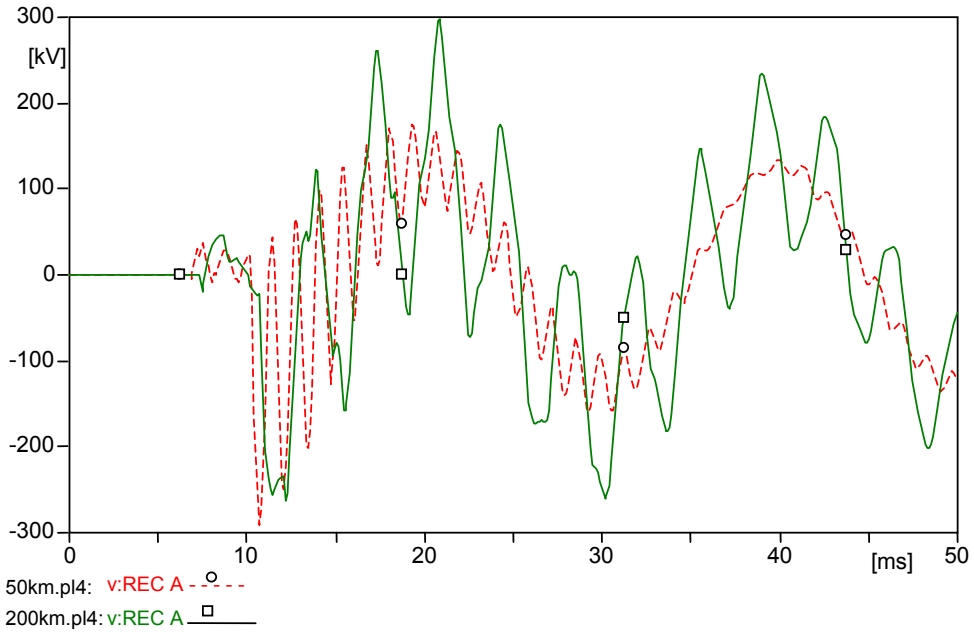

Figure 2.22 Comparison of receiving end voltages of lines of different lengths: 50,200 km

Table 2.2 Overvoltage variations of transmission lines due to lengths

Line	Measurement point	Mean value in pu	Max. values in pu
50 km line	Receiving end	2.1675 pu	2.5 pu
50 km line	At all nodes	2.254 pu	2.5 pu
100 km line	Receiving end	2.208 pu	2.5 pu
100 km line	At all nodes	2.288 pu	2.5 pu
150 km line	Receiving end	2.1415 pu	2.55 pu
150 km line	At all nodes	2.2545 pu	2.55 pu
200 km line	Receiving end	2.082 pu	2.6 pu
200 km line	At all nodes	2.2695 pu	2.6 pu

With the increment of line length, the energization overvoltages determined at the receiving end of the lines are increased thus reaching up to 2.6 pu..

2.4.3 The effect of line source inductance during energization

95.3 mH corresponds to typical value expected in a 154 kV system. The other values assumed are half and 1.5 times of the original value, i.e. 142.95 mH and 47.65 mH. With increment and decrease of the inductance an increase of the voltage is observed.

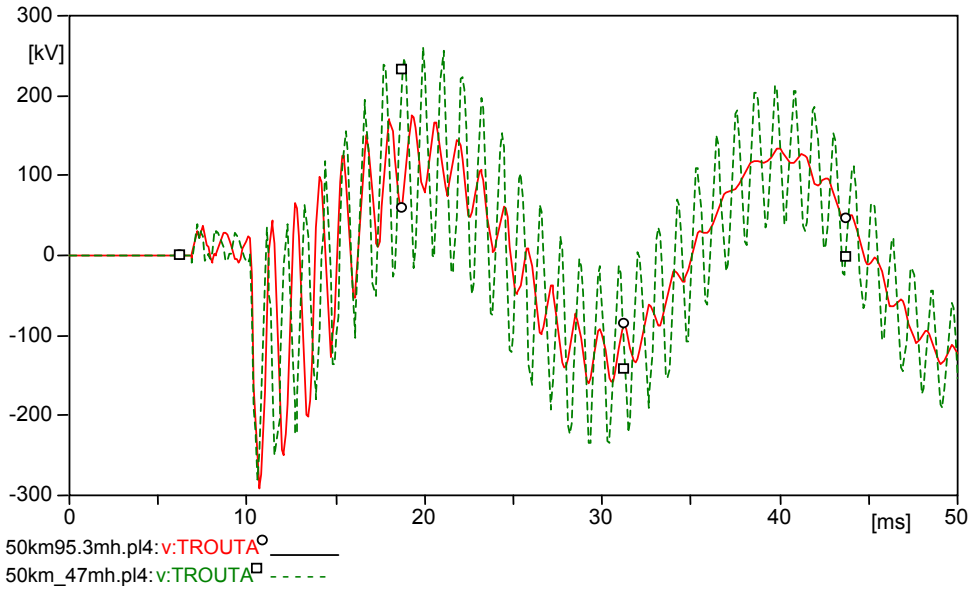

Figure 2.23 Comparison of different source inductances: 95.3, 47.65 mH

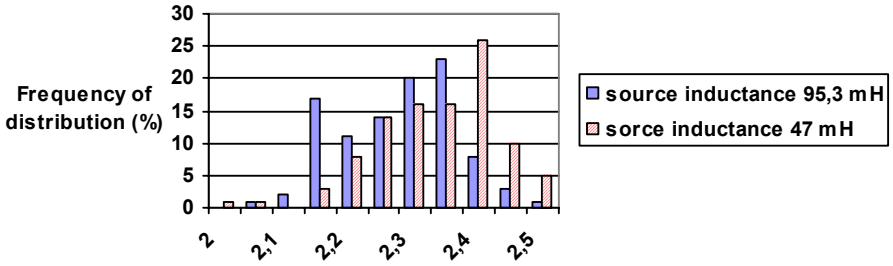

Figure 2.24 Comparison of frequency of occurrence of overvoltages for different source inductances

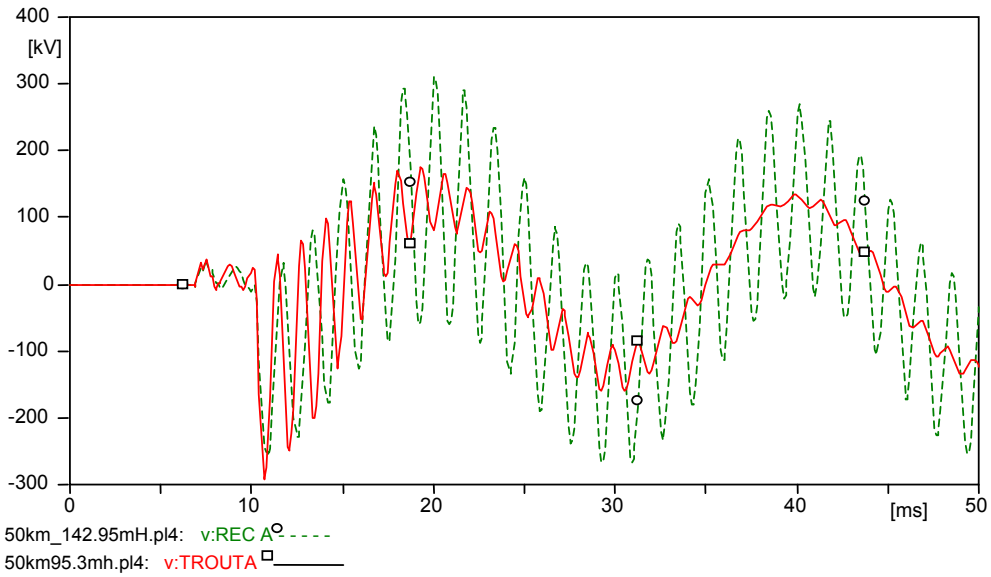

Figure 2.25 Comparison of different source inductances: 95.3, 142.95 mH

Due to results of the cases it can be deduced that decrease of source inductance has an increasing effect on overvoltages. This is due to fact that the higher the source induction the higher will be positive reflection coefficient at the sending end of the system.

2.5 RE-ENERGIZATION ANALYSIS

The need for high speed automatic reclosing is to restore a circuit to service that has been interrupted because of a fault on the line. It is well-known that when interrupting any phase of an AC transmission line that is open circuited at the receiving end, the energy stored in the electrostatic dielectrics at the moment of interruption remains trapped on the transmission line. Therefore, reclosing on a trapped charge, a situation which resembles the strike problem during de-energization of transmission lines, produces switching surges of highest magnitude if no means are taken.

In these sections, first the nature of the trapped charge will be discussed briefly, and then its effects on the energization of lines will be examined through simulations taking into consideration change of line length and source inductance.

2.5.1 NATURE OF TRAPPED CHARGES

The three residual voltages on the phases of the transmission line have different values in relation to the transient phenomena during the opening of the faulted line which determine the initial magnitudes and, the discharge time constant of the line and the time interval between opening and reclosing, determining the final values. The magnitude of the overvoltages produced in the case of a reclosure depends on the magnitude of the trapped charge on the line and also on the point of the supply voltage at which the line is closed. Studies indicate that the higher surge magnitudes are obtained when the circuit breaker closes on phase opposition, with the maximum at the supply wave peak, while for cases closing at the same polarity, there is a reduction compared with the dead line energization. Because the circuit breaker opens at a current zero, the voltage of this time is at its peak value. Therefore, the trapped charges are simulated with distribution of 1,-1,-1 pu voltage on the lines.

2.5.2 SIMULATION RESULTS

EMTP is again used to express re-energization and compare with energization studies. Below is given a figure as a statement of energization and re-energization voltages of 50 km transmission line which was introduced in previous parts.

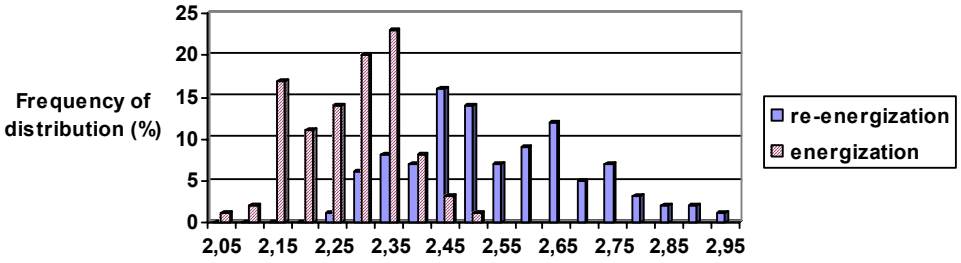

Figure 2.26 Histogram of the distribution of peak overvoltages among all output nodes of the 50 km line (A comparison of energization/ re-energization overvoltages)

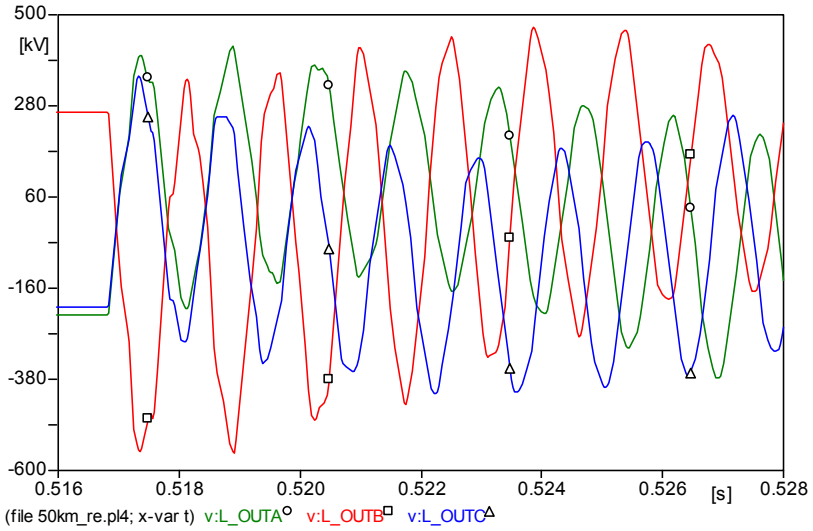

Figure 2.27 Re-energization overvoltages of 50 km line

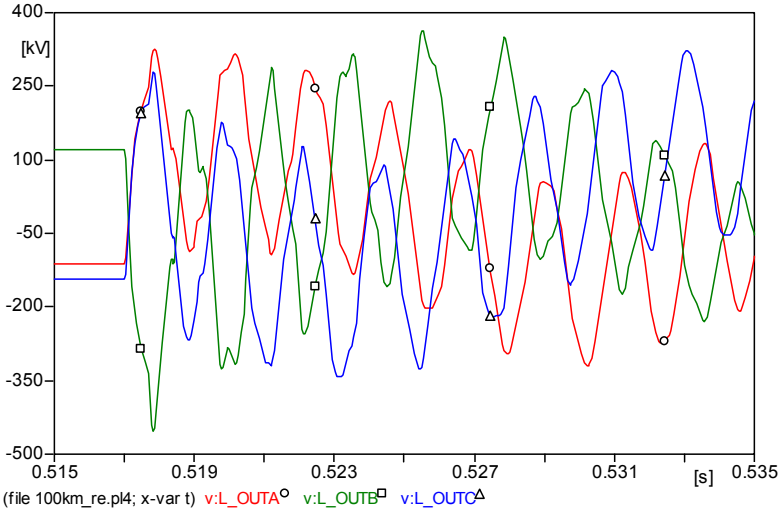

Figure 2.28 Re-energization overvoltages at the receiving end of 100 km line

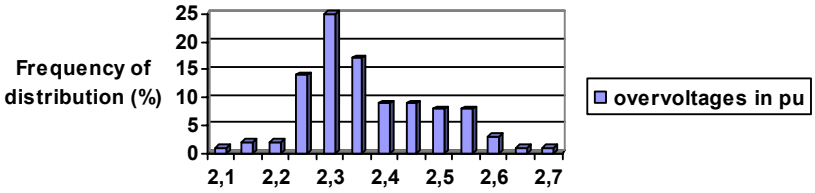

Figure 2.29 Frequency of occurrence of re-energization overvolyages in pu values in phase B at the receiving end of 100 km line

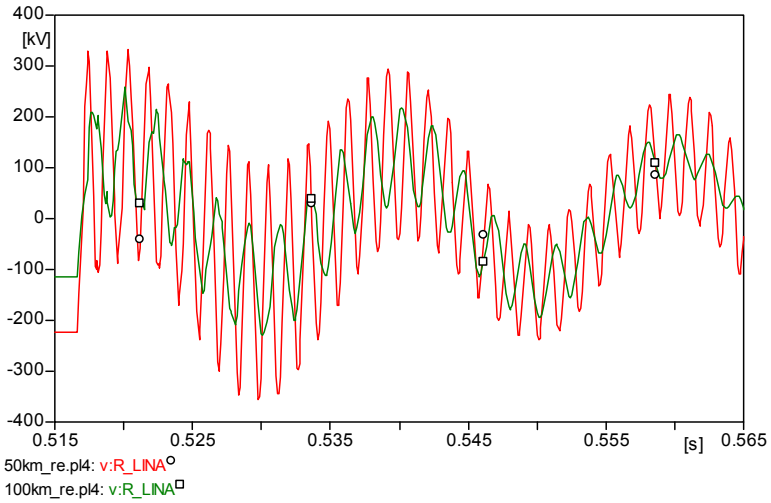

Figure 2.30 Comparison of re-energization overvoltages of 50 km and 100 km lines

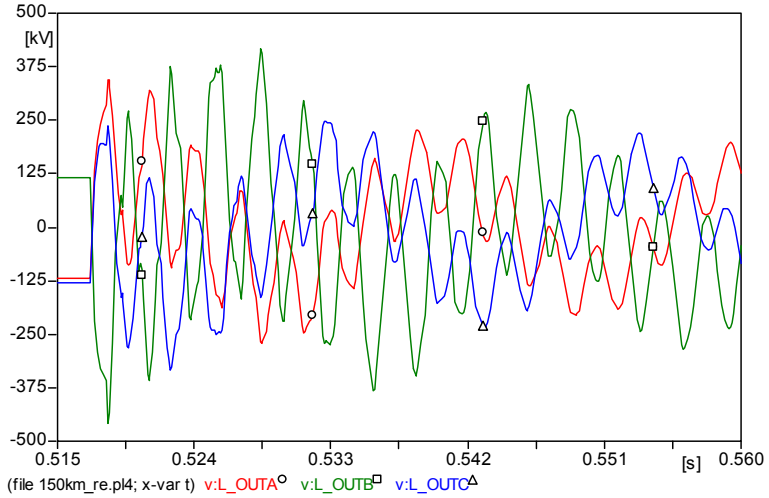

Figure 2.31 Re-energization overvoltages at the receiving end of 150 km line

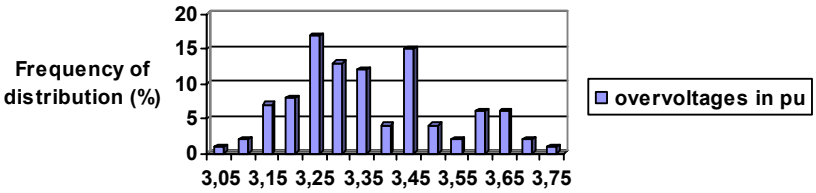

Figure 2.32 Histogram of the distribution of peak overvoltages among all output nodes of the 150 km line

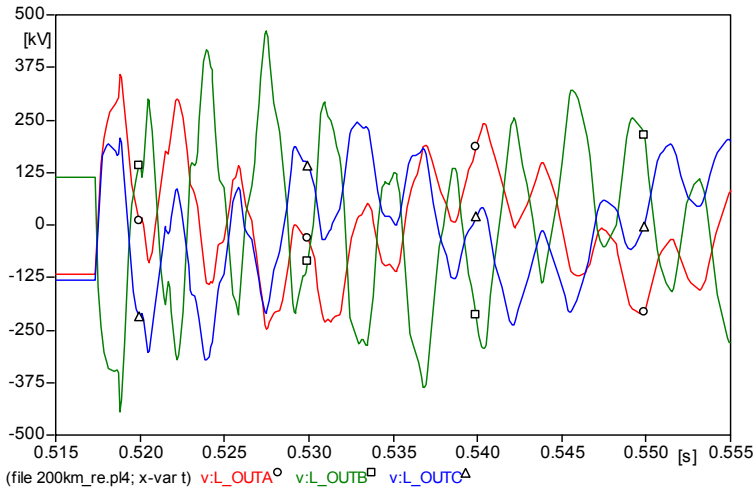

Figure 2.33 Re-energization overvoltages at the receiving end of 200 km line

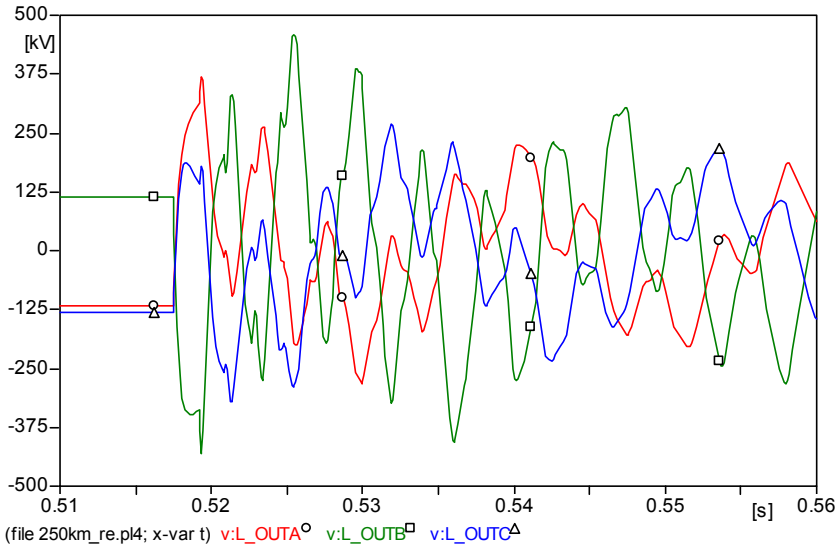

Figure 2.34 Re-energization overvoltages at the receiving end of 250 km line

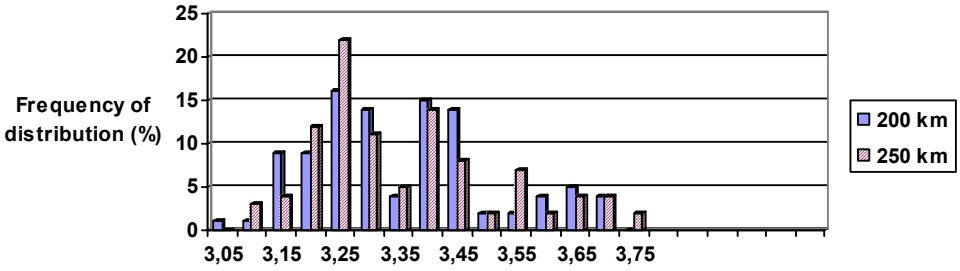

Figure 2.35 A comparison of frequency of occurrence of re-energization overvoltages at the receiving end of 200 and 250 km lines

It can be seen from the results that re-energization results in very high voltage generated in the transmission lines when compared with those cases of transmission line energization, the mean value of the expected overvoltage increases from 2.55 pu to 3.70 pu roughly 43.13 %. The maximum values are again increased to 3.75 in the case of long lines.

This is unacceptable because it will require a very high insulation level which is not going to be economic. Therefore they must be reduced to practical levels, which is the subject of the next chapter.

CHAPTER 3

MEANS OF REDUCTION OF SWITCHING SURGES

3.1 INTRODUCTION

The results of previous chapter show that, the overvoltages generated especially in re-energization transients are quite high and certainly can not be tolerated in a practical line design. Since they will give rise to insulation failures.

The problem of reducing the probability of insulation failure due to stresses arising from energization of transmission lines may be tackled in one or more of the following:

1. Increasing the insulation level, and thereby reducing the probability that a stress causes insulation failure.
2. Reducing the maximum surge levels generated by these switching surges by using specially designed circuit breakers.
3. Introducing a lightning arrester which would prevent the insulation failure by sparking over and reduce the stress.

Clearly, the first alternative is not economical and is out of question and various means of employing the second alternative is considered in next section. Finally, the application of surge arresters in reducing stresses due to switching surges on the transmission lines will be discussed. For such an application, the name “surge diverter” would be more proper.

3.2 RESISTOR ENERGIZATION

Reduction of switching overvoltages in EHV systems can be accomplished by utilizing closing resistors across the circuit breaker contacts at each end of the line. The closing resistors stay in the circuit about 10 msec, which is sufficiently to make sure that transients die away during this time. Generally, the size of the closing resistors is selected as 0.8 and 1.0 pu of the surge impedance of the line, which give adequate results. The operation principle of closing resistors in the circuits is given in Figure 3.1.

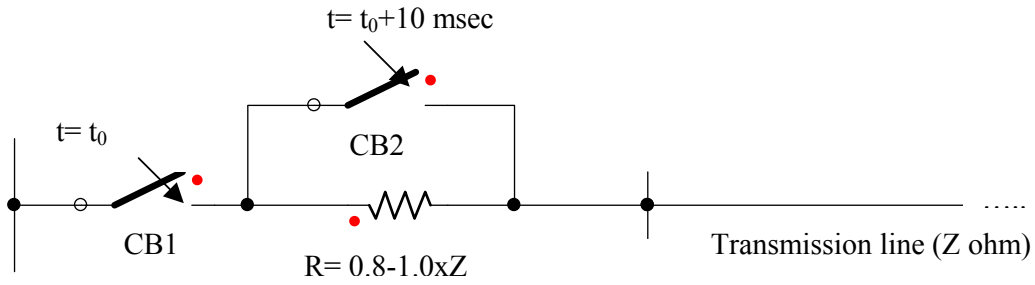

Figure 3.1 The operation principle of closing resistors

During switching operations, CB1 seen in the figure is closed firstly, and the waves start to travel through closing resistors (R). After about 10 msec, the closing resistors are taken out from the circuit by closing CB2, whose contacts are parallel connected to closing resistors.

Thus, the energization taken place in two stages, effectively reducing the maximum value of surge voltages to about 2.7 pu, which can be considered to be an economical level for line insulation.

However, in 1980s some companies began to experience problems with the closing resistor mechanisms in some of the earlier 550 kV SF_6 power circuit breakers installed on the system. [5] A breaker failure resulting from breakdown of a closing resistor operating mechanism caused experts to inspect the

mechanisms of all of the 550 kV power circuit breakers. A large percentage of the circuit breakers were found to have broken failing closing resistor mechanisms. The first reaction in company was to order parts to rebuild the closing resistor mechanisms. However, a growing concern about the reliability of resistors and the possible adverse impact upon power system reliability caused to look for other alternatives.

Fortunately, by 1986 the company was completing a project that replaced all 550 kV line terminal adjustable spill gaps with 396 kV metal oxide (MOV) surge arrester. This project had been motivated by reliability and personnel safety reasons unrelated to the performance of the closing resistors. Now, faced with the potential malfunction of the breaker resistor pre-insertion mechanisms an attractive alternative was to remove these resistors and count on the unique characteristics of the MOV arresters to attenuate the magnitude of the switching surges. [5]

3.3 APPLICATION OF LIGHTNING ARRESTERS

The classical philosophy in the utilization of lightning arresters in insulation coordination has been to protect the terminal apparatus from lightning overvoltages, rather than transmission lines.

To protect generators, transformers, cables, SF_6 buses, and other devices against levels of overvoltages which could permanently destroy their non-self-restoring insulation, surge arresters are installed as close as possible to the protected device. Short connections are important to avoid the doubling effect of traveling waves on open ended lines, even if they are short busses. Surge arresters have normally not been used for the protection of transmission lines, because one can easily recover from insulator flashovers with fast opening and reclosing of circuit breakers (self-restoring insulation), if the overvoltages were due to atmospheric origin.
Protective gaps are seldom used nowadays, except in the protection of series capacitor stations.

The protection of line insulation with arresters in the lower voltage systems for which the overvoltages due to lightning discharges have been the dominant factor in the determination of insulation levels, would have been impracticable in that because the source of overvoltage can be at any part of the line and because of their extremely short wavefronts, voltages within a short distance from the arrester can achieve higher magnitudes than that held by the arrester. These would have necessitated installation of arresters practically at each tower along the line which, obviously, would have been too expensive. However, in contrast, switching surge overvoltages due to line energization can be characterized as possessing wave fronts much longer than those produced by lightning, practically covering the entire line length, and there is a definite source of overvoltages which is the open end of the line where the doubling effect takes place. Therefore it is possible to control the magnitude of overvoltages by placing an arrester at the open end of the line which would sparkover before the overvoltage magnitudes reach a certain level and discharge some of the energy to the ground before they are reflected back to the sending end.

For this application, arresters must have such characteristics that the sparkover and discharge voltages are much less than the desirable surge level of the line. This would require specially designed arresters to meet the conflicting requirements of low switching protective level and ability to withstand severe sustained and/or dynamic voltages, as well as high energy dissipating capabilities.

On a system that has the natural point solidly grounded which is the case for EHV systems, and assuming that there are no dynamic voltages, the highest sustained over voltages would be those due to the occurrence of a single line to ground fault on one of the other phases. [4] To a first degree of approximation, it can be shown by using symmetrical components that in such a case the voltage across the arresters on the healthy phases is given by

$$e = \frac{\sqrt{3}}{2} E \left[\frac{\sqrt{3}(Z_0 + R) + j(Z_0 + 2Z_1 + 3R)}{Z_0 + 2Z_1 + 3R} \right]$$

Equation 3.1

where Z_0= zero sequence impedance

Z_1= positive sequence impedance which is equal to the negative sequence impedance

R= fault resistance

and E= the maximum system voltage

An important parameter to define the surge arrester is the protection level (V_p) which is residual voltage across the arrester during the passage of a defined current surge, called nominal discharge current. For switching impulses the nominal discharge current value is normally about 1 to 2 kA.

The energy absorbed is another important parameter to be considered due to its correlation with the thermal stability of the arrester. It's a function of the switching overvoltages, protection level of the arresters and line characteristics. The high energy dissipation capability of modern ZnO surge-arresters normally copes with the line switching requirements even for the long lines.

3.3.1 SiC ARRESTERS

There are two basic types of surge arresters, namely silicon-carbide surge arresters, and metal-oxide surge arresters. Until about 15 years ago, only silicone-carbide arresters were used, but the metal-oxide arrester has quickly replaced the older type to the extent that some manufacturers produce only metal-oxide arresters now.

Silicon-carbide arresters consist of a silicon-carbide resistor with a nonlinear v-i characteristic, in series with a spark gap to avoid excessive currents during normal operation. When voltage exceeds a certain threshold, the air gap arcs over and voltage is clamped across the arrester. The spark gap connects the arrester to the system when the overvoltage exceeds the sparkover voltage, and the resistor limits the following current and enables the arrester to "reseal" (interrupt the current in the gap). To facilitate resealing, so-called "active spark gaps" have been designed

in which an arc voltage builds up after sometime. A resistor block in series with the gap is not very high (typically 4 cm), and to produce the desired sparkover voltage and nonlinear resistance for a particular voltage level, many such blocks are stacked together in a series connection. To achieve a reasonably uniform voltage distribution along the stack, parallel R-C grading networks are used, which are normally ignored in EMTP simulations. [6]

Silicon carbide arresters tend to fail more often than MOVs due to the presence of air gaps. Moisture entering an air gap can cause corrosion and reduce the voltage withstand strength of the gap. Further, thermal expansion of water vapor under heat can result in damaging mechanical stress to the interior of the arrester and can result in catastrophic failure during normal or overvoltage situations. Other failure modes include bad or aged blocks and direct lightning strikes. There are four other major failure modes associated with surge arresters: puncture, thermal runaway, cracking under tension and cracking under compression. Cracking and puncture are caused by a localization of the current, which causes concentrated heating leading to nonuniform thermal expansion and thermal stresses. Puncture is most likely in varistor disks with low geometrical aspect ratio, when the current density has intermediate values. Cracking dominates at higher current densities and for disks with high aspect ratio. Puncture and cracking do not occur when the current is small, because the time evolution of the nonuniform heating is slow enough for the temperature distribution to flatten. For low and very high current densities, the most likely failure mode is thermal runaway— the surge arrester simply is not able to handle the energy levels flowing through it.

To ensure proper selection, we must know which type of lightning arrester to use and what its rating means. IEEE C62.1 Standard for Gapped Silicon Surge Arresters for AC Power Circuits applies to gapped silicon-carbide surge-protective devices designed for repeated limiting of voltage surges on 50 Hz or 60 Hz power circuits by passing surge discharge current and subsequently automatically interrupting the flow of follow current. Within this standard various tests are introduced to put forward the insulation and protective characteristics of arresters.

Arrester classification is determined by prescribed test requirements. These classifications are:

- station arrester
- intermediate arrester
- distribution arrester
- secondary arrester

A metal oxide varistor has two ratings; duty cycle and maximum continous operating voltage. SiC arrester has just the duty cycle rating (in kV) which duty cycle testing established. The duty-cycle test serves to establish the ability of the arrester to interrupt follow current successfully and repeatedly under specified conditions. [6]

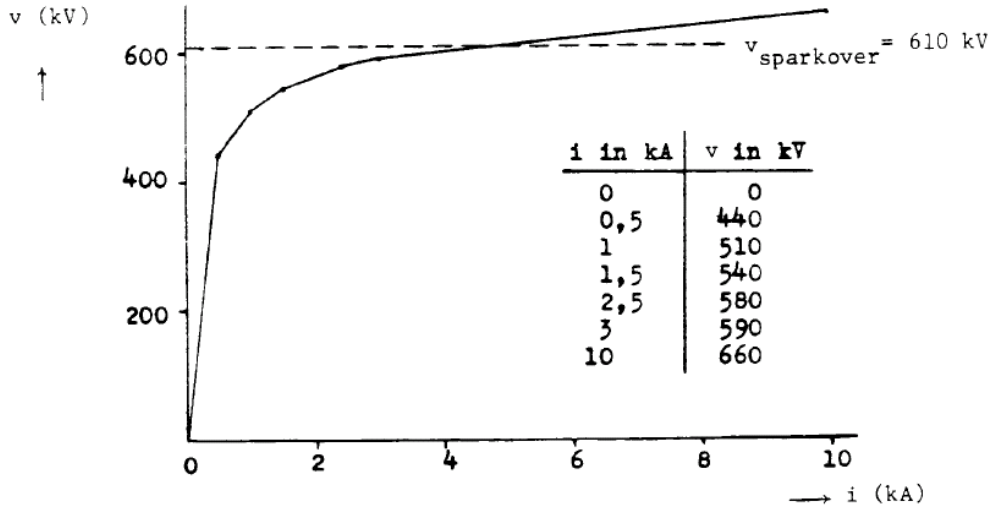

Figure 3.2 Nonlinear characteristic of a 220 kV silicon-carbide surge arrester

Silicon-carbide arresters are modeled in the EMTP as a nonlinear resistance in series with a gap which has a constant sparkover voltage. In reality the sparkover voltage depends on the steepness of the incoming wave, as shown in figure 3.4. since surge in a system have very irregular shapes, rather than a linear rise. Therefore, it is not easy to implement the steepness dependence of the sparkover voltage.

In silicon-carbide surge arresters with current-limiting gaps, a voltage builds up across the gap after 200 to 400 μs, which is the best modeled as an inserted ramp-type voltage source. This gap voltage is only important in switching surge studies. In lightning surge studies it can be ignored because of the time delay of 200 to 400μs.

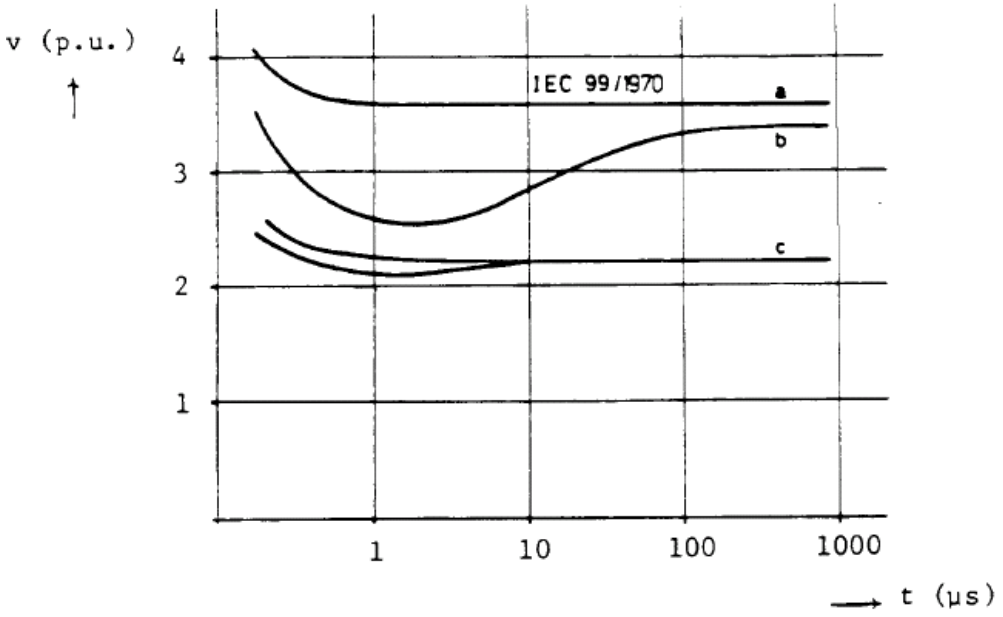

a= medium voltage

b= high voltage, lightning surge protection

c = high voltage, lightning and switching surge protection

Figure 3.3 Arrester sparkover voltage time characteristic for wave fronts with linear rise

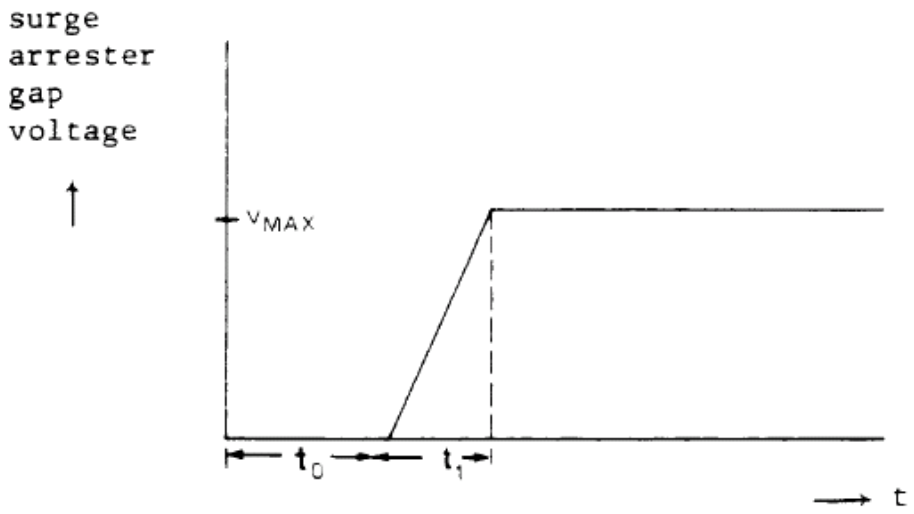

Figure 3.4 Arrester gap characteristic

3.3.2 ZnO ARRESTERS

Metal oxide varistors (MOVs) have a highly nonlinear resistance (as a function of voltage), do not conduct excessive currents during normal operation, and generally do not require an air gap. When voltage exceeds a certain threshold, the resistance of the MOV drops sharply and clamps voltage across the device (similar to a Zener diode).

The installation of surge arresters at the line terminals is another method widely applied in high and extra high voltage networks. It offers several advantages over the old silicon carbide (SiC) arresters. Metal Oxide (ZnO) surge arresters are non-linear resistive elements, in which the voltage across their terminals is a function of the current flowing through them. For the normal operation voltage level the arresters have an extremely high resistance. Above a certain voltage level they start to drain current from the network. In summary improved durability, higher energy handling capabilities, elimination of front of wave sparkover, improved contamination performance and stability of protective characteristics have been the key reasons why this technology is accepted by utilities. [7,8]

Metal-oxide or zinc-oxide surge arresters are highly nonlinear resistors, with an almost infinite slope in the normal-voltage region, and an almost horizontal slope in the overvoltage protection region as shown in Figure 3.5.

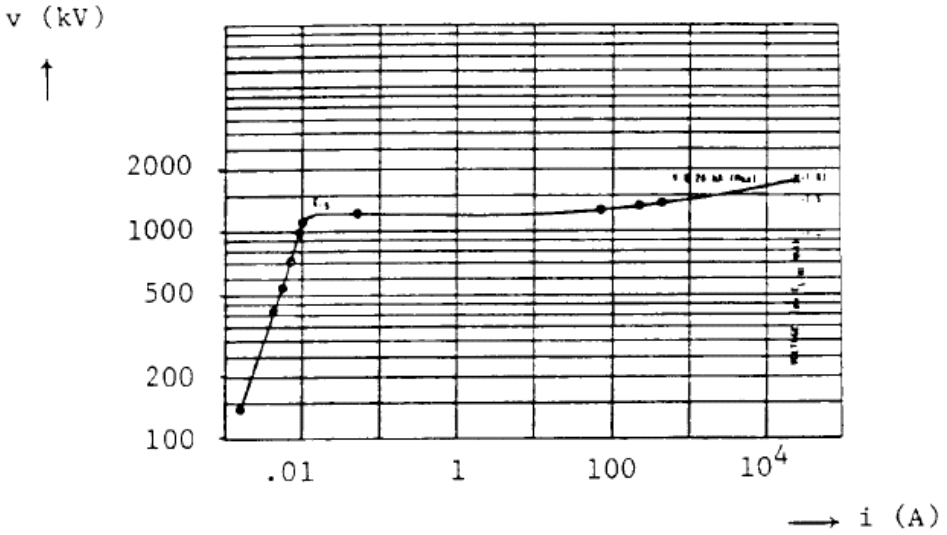

Figure 3.5 Voltage-current characteristic of a 1200 kV gapless metal-oxide surge arrester

They were originally gapless, but some manufacturers have re-introduced gaps into the design. Its nonlinear resistance is represented by an exponential term as follows:

$$I = p \times \left(\frac{V}{V_{REF}} \right)^{q} \qquad \text{Equation 3.2}$$

Where "I" is the arrester current (discharge current in amper), "V" is the voltage applied across the arrester (residual voltage in volts), and p and q are the constants of the device (typical values for q = 20 to 30). This equation is accurate when "I" is in the range of 500 A to 3000 A, which is the case in the switching operations. This non-linear relation between the discharge current and residual voltage of a surge arrester can be formed by ATP supporting routine called ZNO FITTER. The

non-linear V-I characteristics is approximated by an arbitrary number of exponential segments by this routine. [1] Since it is difficult to describe the entire region with one power function, the voltage region has been divided into segments in the BPA EMTP, with each segment defined by its own function. In the UBC EMTP, only one function is allowed so far. For voltages substantially below V_{ref}, the current is extremely small (e.g., $I = p.0.5^{30} = p.10^{-9}$ for $V/V_{ref} = 0.5$) and a linear representation is therefore used in this low voltage region. In the meaningful overvoltage protection region, two segments with power functions are usually sufficient.

The static characteristic of Eq.3.2 can be extended to include dynamic characteristics similar to hysteresis effects, through the addition of a series inductance L, whose value can be estimated once the arrester current is approximately known from a trial run. A metal-oxide surge arrester model for fast front current surges with time to crest in the range of 0.5 to 10 μs was proposed and compared against laboratory tests by Durbak. [5] The basic idea is to divide the single nonlinear resistance into m parallel nonlinear resistances, which are separated by 2 low pass filters as illustrated in Figure 3.6 for two parallel nonlinearities, which is usually sufficient in practice. The R_1-L_1 circuit is the low pass filter which separates the two nonlinear resistances defined by $i_0(V_0)$ and $i_1(V_1)$. The inductance L_0 represents the small but finite inductance associated with the magnetic fields in the immediate vicinity of the surge arrester, while R_0 is used only to damp numerical oscillations. C is the stray capacitance of the surge arrester. The model of figure 3.6 can easily be created from existing EMTP elements. If three such models were connected to phases a, b, c , then the six nonlinear resistances would have to be solved with the compensation method with a six phase Thevenin equivalent circuit.

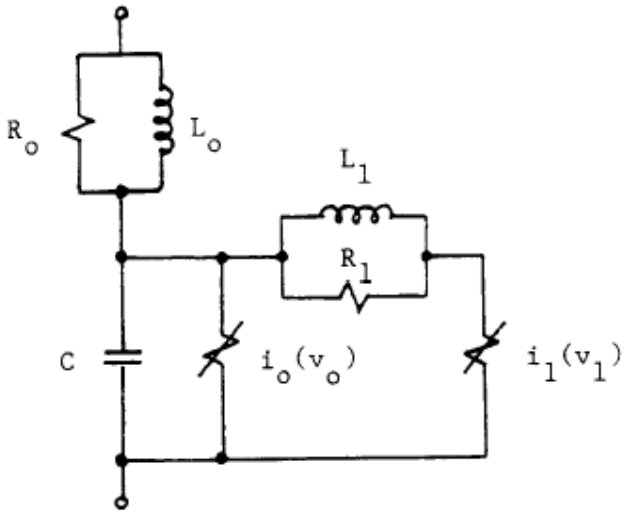

Figure 3.6 Two-section surge arrester model for fast front surges

A somewhat different model has been proposed by Knecht [1]. It consists of a nonlinear resistance R(v), a more or less constant capacitance C, and a linear, but frequency-dependant impedance Z(w).

No IEEE guidelines have ye been published for the modeling of metal-oxide surge arrester. The energy absorbed in them is an important design factor, and should therefore be computed in whatever type of model is used. Since energy absorption may change as the system is expanded, it is important to check whether ratings which were appropriate initially may possibly exceeded in future years. Energy absorption capability is probably more of a limitation for switching surges than for lightning surges. The sharp change from the almost vertical to the almost horizontal slope, which limits overvoltages almost ideally at the arrester location, could produce oscillations with overshoot at locations some distance from the arrester, especially in substations with long bus runs. This may be another factor worth watching for.

Metal-oxide surge arresters are generally solved with the compensation method in the EMTP, with iterations using Newton's method. The piecewise linear representation is less useful because the highly nonlinear characteristics of Eq. 3.2 is not easily described by piecewise linear segments.

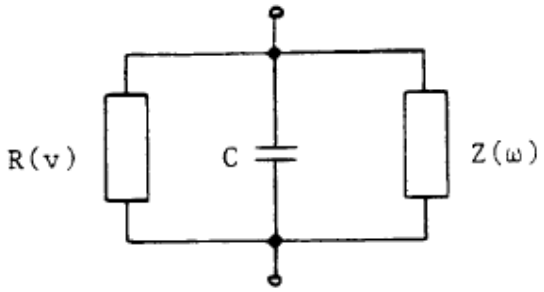

Figure 3.7 Alternative surge arrester model

If the surge arrester is equipped with a shunt spark gap, as illustrated in Fig.3.8, then it is still represented as a nonlinear resistance in the solution process except that the function for the resistance will change abruptly from $R_1(i) + R_2(i)$ to represent the series gap before sparkover.

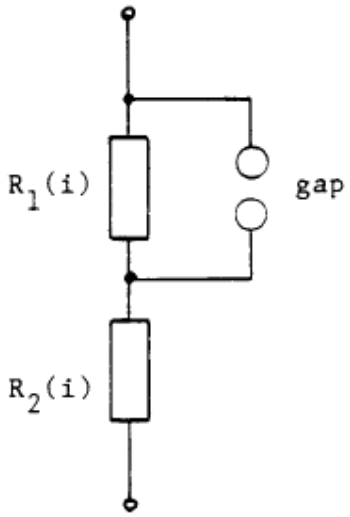

Figure 3.8 Metal-oxide surge arrester with shunt spark gap

3.3.3 Selection of Surge Arresters

Selection of the proper arrester is very important and carried in two steps;

- Matching the electrical characteristics of the arresters to the system's electrical demands
- Matching the mechanical characteristics of the arresters to the system's mechanical and environmental requirements.

In order to reduce the risk of insulation failure to an economically and operationally acceptable level, the insulation withstand of substation equipment is selected with regard to expected overvoltages, taking into account the protective characteristics of the surge arresters. The insulation withstand of the surge arrester itself has to be coordinated with its own protective characteristics. The arrester has to be positioned with respect to grounded objects and surge arresters in adjacent phases, without increasing the total risk for insulation failure. The insulation withstand properties of surge arresters in a substation can be divided into:

- Withstand of the surge arrester itself, including the insulation between flanges and grading rings, etc.
- Insulation withstand between the surge arrester and grounded objects.
- Insulation withstand between the surge arrester and other equipment connected to the same phase, e.g. bushings.
- Insulation withstand between surge arresters in adjacent phases. [9]

The advantage of these arresters is their increased limitation and reliability compared with silicon carbide arresters.

CHAPTER 4

OVERVOLTAGE PROTECTION BY SURGE ARRESTER

4.1 INTRODUCTION

The result and evaluations of the switching surges arising both energization and re-energization studies have shown that the system could be subjected to unacceptable overvoltage stresses. In the previous chapter, reduction methods of these overvoltages are introduced which were resistor switching and utilization of surge arresters.

Installation of surge arresters at appropriate locations of the electrical system has now become the standard procedure and is applied for the protection of the lines against switching and lightning overvoltages.

This chapter describes the overvoltages reduction method via the application of Metal Oxide (ZnO) surge arresters at appropriate locations of a system that will be studied in this chapter, and determines the optimum number of surge arresters required focusing on the energy absorption levels of the arresters. First, the system modelling and application of surge arresters is given in Section 4.2, followed by the simulation results of utilization of surges at different parts of the line in Section 4.3. Finally, Section 4.4 describes the evaluation of computer simulation studies.

4.2 APPLICATION OF METAL OXIDE (ZnO) SURGE ARRESTER

4.2.1 SYSTEM MODELLED

The part of the transmission line which is between Hopa and Enguri is energized from Hopa side by source representing trap source by 180 kV and then re-energized from Enguri side with an identical source. Line lengths are 19.5 km Hopa-Border, 12.3 km Border-Batum, 160 km Batum-Vardnili, 15 km Vardnili-Enguri. First simulation is carried out without any surge arrester. The following ones are executed by one arrester, 2 arresters at different nodes and 3 arresters used at the different ends of the line will be examined in order to study the effect of location of surge arresters. To be able to compare the results another simulation is carried out for energizing from Enguri side and re-energization from Hopa side.

4.3 RE-ENERGIZATION SIMULATIONS AND UTILIZATION OF SURGE ARRESTERS AT DIFFERENT LOCATIONS

4.3.1 Simulation of re-energization of Hopa-Enguri transmission line from Enguri side without arresters (case 1)

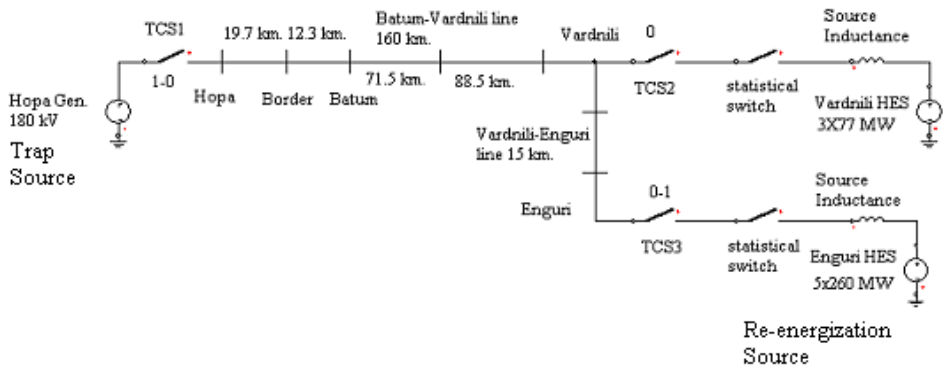

Figure 4.1 Transmission line configuration (no arrester is used)

Figure 4.1 is the base case for simulations to investigate the overvoltage reducing effects of surge arresters. Hopa side of the network is described as one single

source of 180 kV. Source inductances of Vardnili and Enguri sources are in turn 138 mH and 38.1 mH. Time controlled switch (TCS1) at Hopa energizes the network from beginning (-1 s.) to 0.01 s., TCS2 remains open and TCS3 re-energizes the network at 0.02s. and will be opened at 10 s.

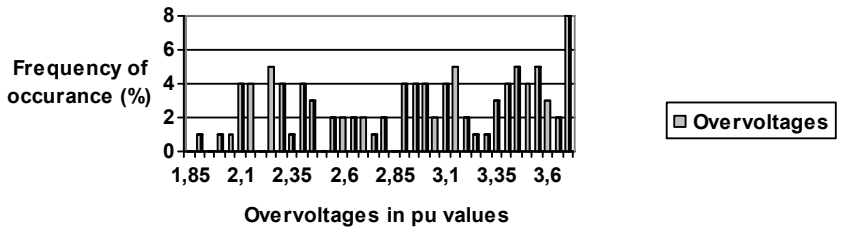

Figure 4.2 Histogram of voltage distribution for the maximum of the peaks at all output nodes. (No arrester is used)

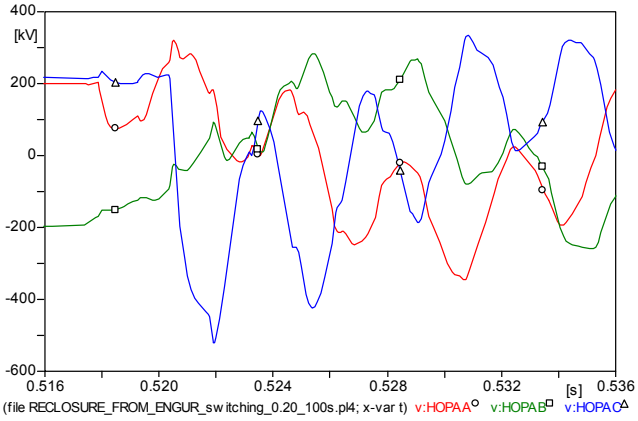

Figure 4.3 Receiving end voltage of line at Hopa (no arrester is used)

Table 4.1 Overvoltages when the system is energized from Hopa and re-energized from Enguri (no arrester is used)

Measurement point	Mean values in pu	Mean values kV	Max values in pu	Max values kV
Hopa phase A	1.775 pu	319.5 kV	2.35 pu	423 kV
Hopa phase B	1.723 pu	310.14 kV	2.15 pu	387 kV
Hopa phase C	2.94 pu	529.2 kV	3.70 pu	666 kV
Enguri phase A	1.31 pu	235.8 kV	1.60 pu	288 kV
Enguri phase B	1.293 pu	232.74 kV	1.5 pu	270 kV
Enguri phase C	1.765 pu	317 kV	2.25 pu	405 kV
All over nodes	2.93 pu	527.4 kV	3.70 pu	666 kV

The statistical distribution as a function of random switch closure of the defined system is given in Figure 4.2. A sample of overvoltages generated is given in Figure 4.3 where re-energization voltages have reached a magnitude of 529.2 kV which is 2.94 pu for phase C, 319.5 kV and 1.7 pu for phase A, 310.14 kV and 1.723 pu for phase B, and from the Programmers File Editor's file, where all output files can be viewed, the maximum peak voltages for Hopa phases are; for phase C 666 kV which is 3.7 pu, for phase A 2.35 pu and 423 kV and for phase B 2.15 pu and 387 kV . In Figure 4.4, histogram of voltage distribution for the maximum of the peaks at Hopa bus phase C is presented where overvoltage values differ between 1.85-3.7 pu.

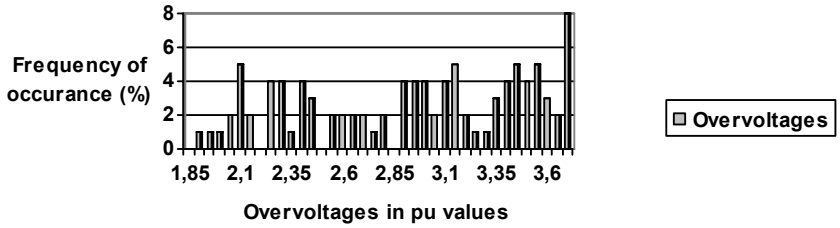

Figure 4.4 Histogram of voltage distribution for the maximum of the peaks at Hopa bus phase C (No arrester is used)

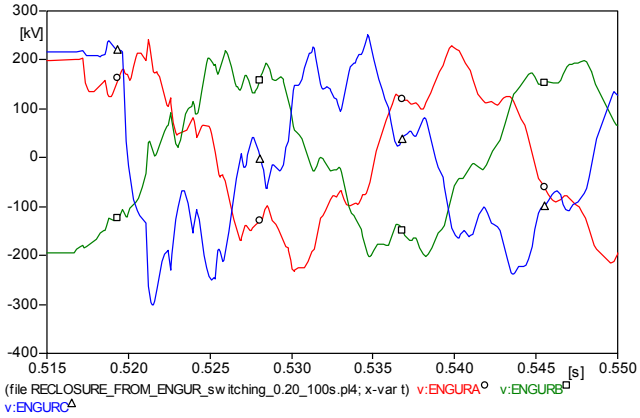

Figure 4.5 Receiving end voltage of line at Enguri (no arrester is used)

The overvoltage values reach up 317 kV at Enguri phase C when the network is re-energized from Hopa is presented in Figure 4.5 and statistical distribution of

overvoltages is depicted in Figure 4.6. Whilst the maximum value in overvoltage distribution histogram reaches to 3.7 pu (% 8) for the Hopa node (the receiving end for re-energization process from Enguri), on the other hand it reaches to only 2.25 pu at Enguri which is the sending end.

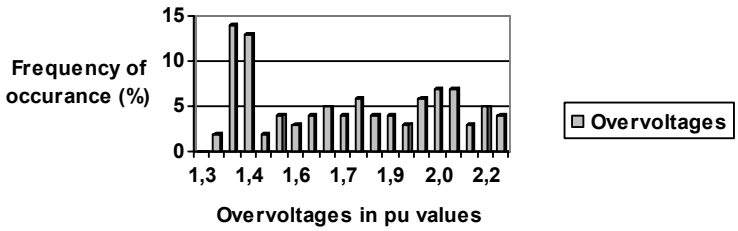

Figure 4.6 Histogram of voltage distribution for the maximum of the peaks at Enguri. (No arrester is used)

4.3.2 Simulation of re-energization of Hopa-Enguri transmission line from Hopa side without arresters (case 2)

For a comparative point of view on results another simulation is carried out for energizing from Enguri side and re-energization from Hopa side. A trapped voltage is given for 0.01 s. and then re-energized at 0.02 s. Hopa bus is supplied with Ardeşen, Rize, Hopa and Artvin generators. Time controlled and statistical switches are again used to simulate energizing and re-energizing processes.

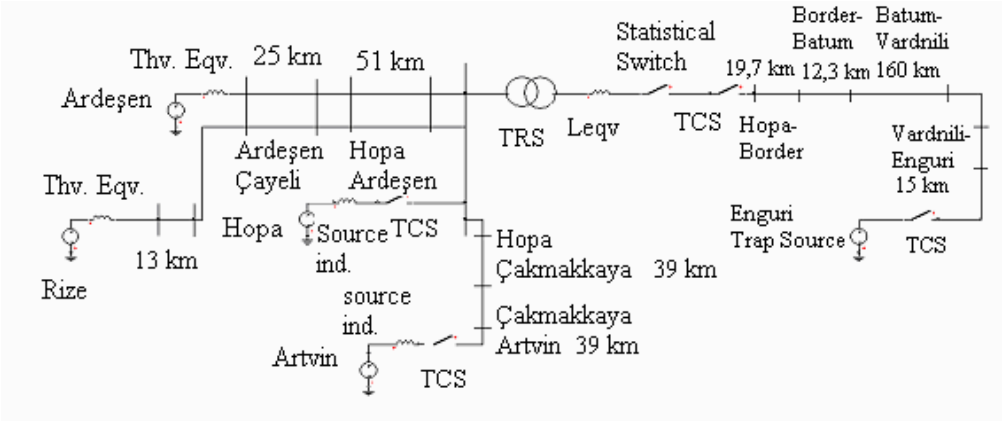

Figure 4.7 Transmission line configuration (no arrester is used)

For this simulation the system is energized from Enguri bus with 180 kV (as the trapped voltage source) and re-energized from Hopa bus. The statistical distribution as a function of random switch closure of the defined system is given in Figure 4.8.

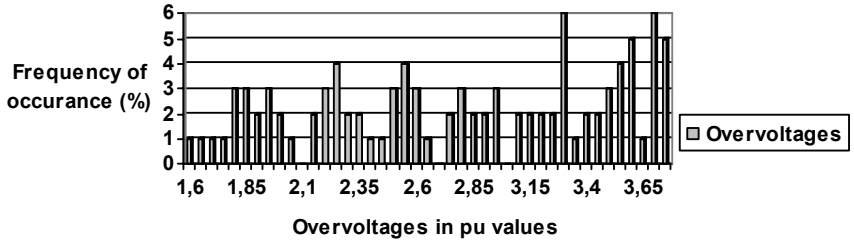

Figure 4.8 Histogram of voltage distribution for the maximum of the peaks at all output nodes. (No arrester is used)

The overvoltage distribution overall nodes for second case shows a similar response with the first case but due to difference of energization and re-energization points distribution of overvoltages at Enguri and Hopa varies. And the overvoltage occurrence frequency at the beginning of the 19.7 km Hopa-Border line for the re-energization from Hopa is given in figure 4.9.And voltage values at Hopa bus is presented in figure 4.10 which reach to 335 kV in the figure.

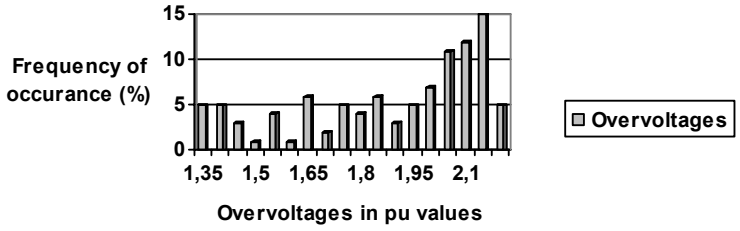

Figure 4.9 Histogram of voltage distribution for the maximum of the peaks at the beginning of Hopa-Border line. (No arrester is used)

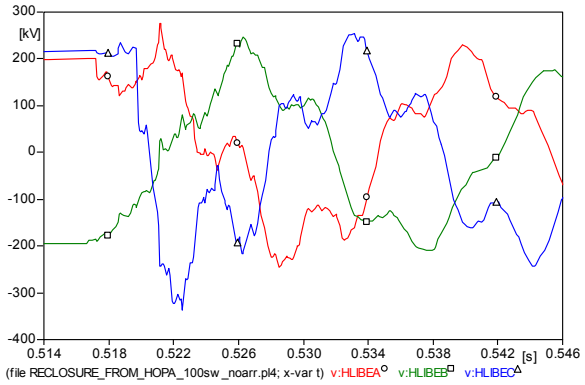

Figure 4.10 Receiving end voltage of line at Enguri (no arrester is used)

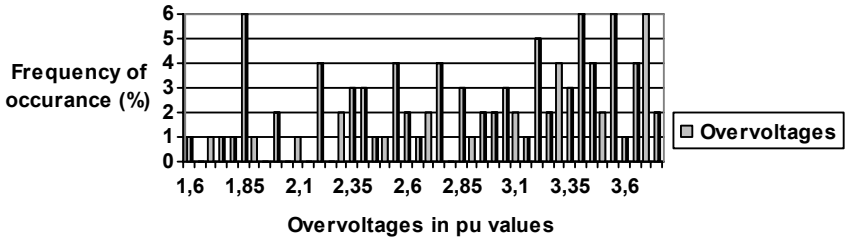

Figure 4.11 Histogram of voltage distribution for the maximum of the peaks Enguri phase C (no arrester is used)

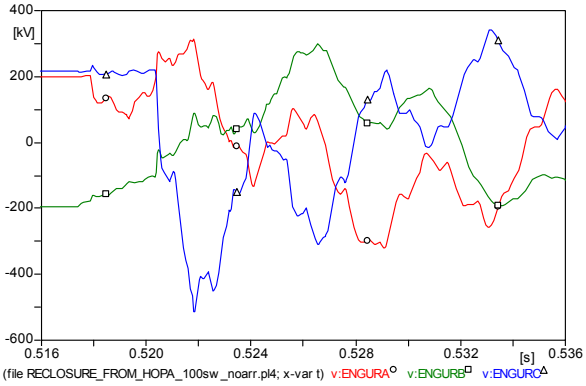

Figure 4.12 Receiving end voltage of line at Enguri (no arrester is used)

A sample of overvoltages generated at Enguri is given in Figure 4.12 where re-energization voltages have reached a magnitude of 515 kV in the figure and in Programmers File Editor's file , where all output files can be viewed, a maximum peak voltage for Enguri Phase C is noticed 675 kV(2%).

Table 4.2 Overvoltages when the system is energized from Hopa and re-energized from Hopa (no arrester is used)

Measurement point	Mean values in pu	Mean values kV	Max values in pu	Max values kV
Hopa phase A	1.4425 pu	259.65 kV	1.70 pu	306 kV
Hopa phase B	1.439 pu	259.02 kV	1.75 pu	315 kV
Hopa phase C	1.857 pu	334.26 kV	2.20 pu	396 kV
Enguri phase A	1.876 pu	337.68 kV	2.5 pu	450 kV
Enguri phase B	1.7995 pu	323.91 kV	2.30 pu	414 kV
Enguri phase C	2.885 pu	519.3 kV	3.75 pu	675 kV
All over nodes	2.905 pu	522.9 kV	3.75 pu	675 kV

When compared with first case it can be deduced that due to energization and re-energization point, bus overvoltages differ. And due to changes in configuration in the second change overvoltages at all nodes have increased.

4.3.3 Simulation with one arrester placed at Hopa (A comparison of re-energization from Enguri and re-energization from Hopa)

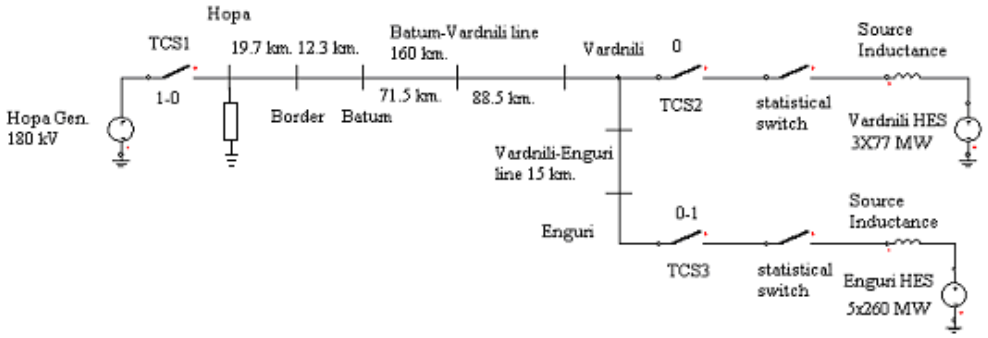

Figure 4.13 Location of the first surge arrester installed at Hopa

Figure 4.13 illustrates the first step application of the arrester sets (along with their locations) simulated in order to determine the optimum number of surge arresters required to protect from overvoltage surges appearing in the HV overhead line system. The time controlled switch at trap source is closed at -1 second and opened at 0.01 s obtaining a trap source on the line. The time controlled switch

after Vardnili bus is opened at -1 s and closed at 10 seconds causing Vardnili generator to be taken out of the system. The time controlled switch at Enguri is closed at 0.02 s. to represent re-energization and is opened at 10 s. Re-energization is simulated by the help of statistical switch to a state the statistical nature of switching. One set of arresters would be sufficient if the line is closed from one end only. If the line can be closed from both ends, then it can be seen that two sets, one at each end is the absolute minimum.

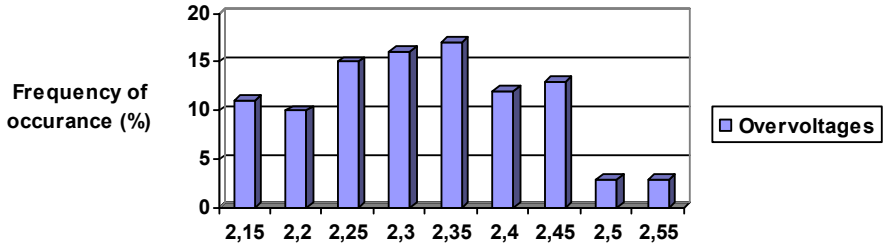

Figure 4.14 Histogram of voltage distribution for the maximum of the peaks at all output nodes when the system energized from Enguri and one arrester is used at Hopa

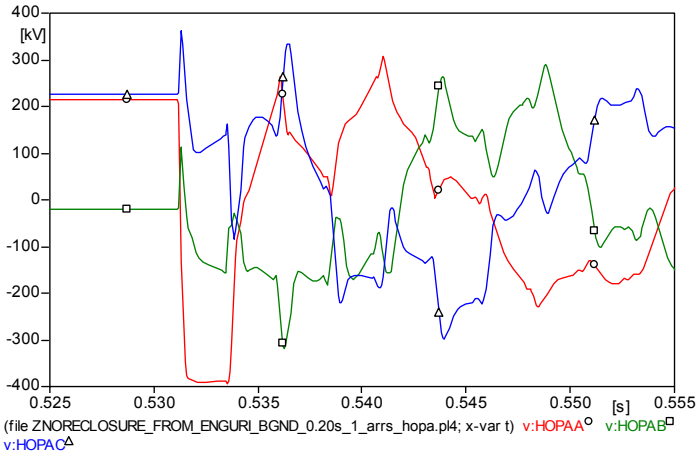

Figure 4.15 Receiving end voltage of line at Hopa when an arrester is used at Hopa

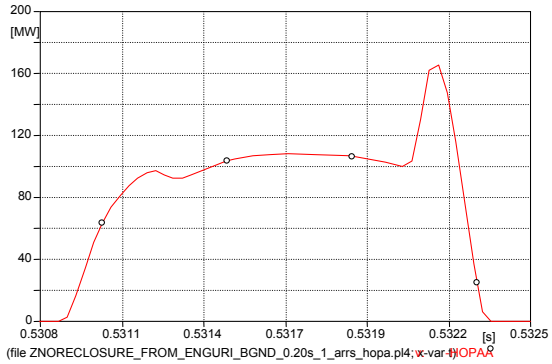

Figure 4.16 Power characteristic of surge arrester at Hopa (phase A)

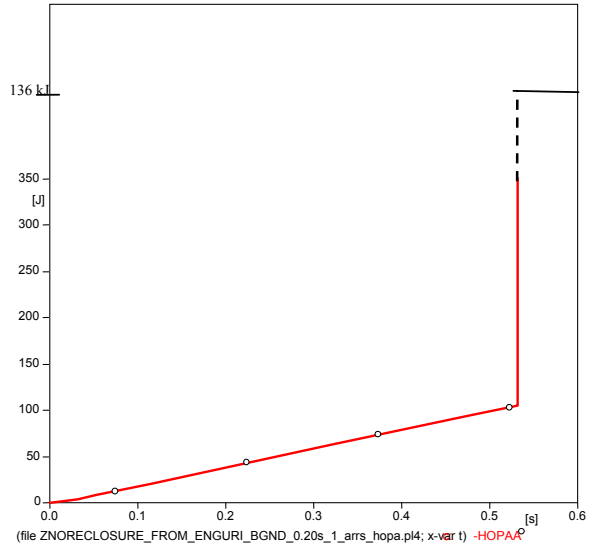

Figure 4.17 Energy absorption characteristic of surge arrester at Hopa when an arrester is used at Hopa (of Phase A)

Table 4.3 Overvoltages when the system is energized from Hopa and re-energized from Enguri (arrester is used at Hopa)

Measurement point	Mean values in pu	Mean values kV	Max values in pu	Max values kV
Hopa phase A	2.218 pu	399.24 kV	2.30 pu	414 kV
Hopa phase B	1.635 pu	294.3 kV	2 pu	360 kV
Hopa phase C	2.0135 pu	362.34 kV	2.15 pu	387 kV
Enguri phase A	1.703 pu	306.54 kV	1.90 pu	342 kV
All over nodes	2.4115 pu	434.07 kV	2.60 pu	468 kV

When compared with the basic case, it is observed that the maximum overvoltage at Hopa has decreased from 529,2 kV to 399 kV. At Enguri it lessens from 2,25 pu to 1,9 pu. And at all output nodes maximum value has decreased from 666 kV to 468 kV with the addition of surge arrester.

In order to perform a comparative study for this case surge arrester is to be studied at Hopa for the network energization from Enguri as the trap source and re-energized from Hopa bus. While in the first simulation without arresters, the overvoltages at Hopa reached up to 3.7 pu and 666 kV, after placement of a surge arrester at the bus this value decreases to 332 kV and 2.1 pu. as presented in Figure 4.18 and 4.19.

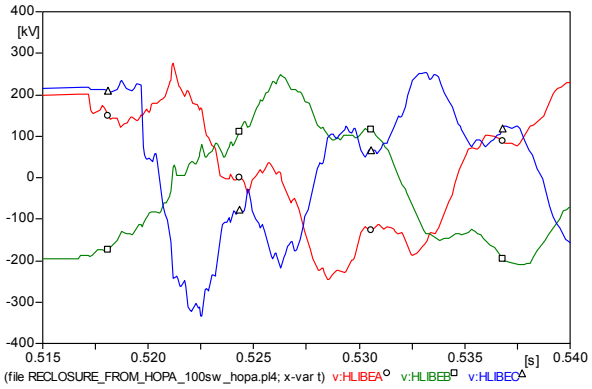

Figure 4.18 Sending end voltage of line at Hopa when an arrester is used at Hopa and line is re-energized from Hopa

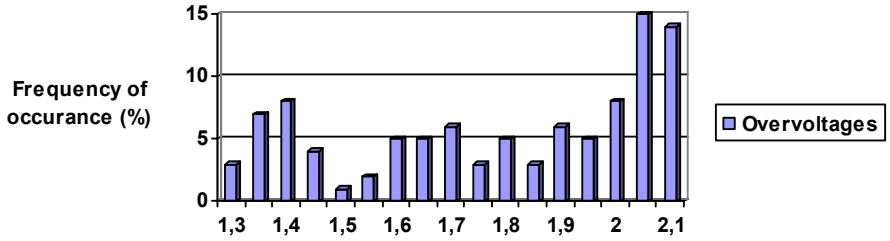

Figure 4.19 Histogram of voltage distribution for the maximum of the peaks of Hopa bus phase C when the system re-energized from Hopa and one arrester is used at Hopa

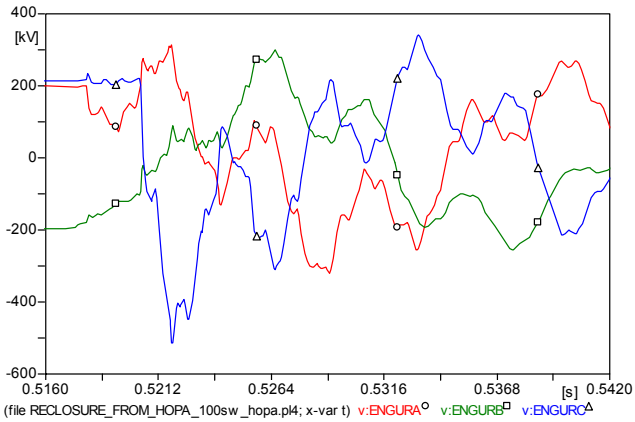

Figure 4.20 Receiving end voltage of line at Enguri when an arrester is used at Hopa and line is re-energized from Hopa

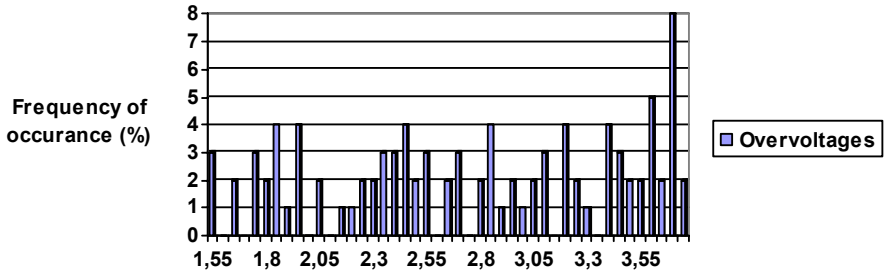

Figure 4.21 Histogram of voltage distribution for the maximum of the peaks of Enguri phase C when the system re-energized from Hopa and one arrester is used at Hopa

When an arrester is placed at Hopa the histogram of overvoltages at all output nodes have decreased from 522,9 kV to 495,36 kV. The voltages at Hopa bus show a slight decrease i.e. from 396 kV to 378 kV.

Power characteristic for this case presents higher peak when compared to the case again with arrester at Hopa but network re-energized from Enguri because the power to be dissipated has increased due to the position of the arrester.

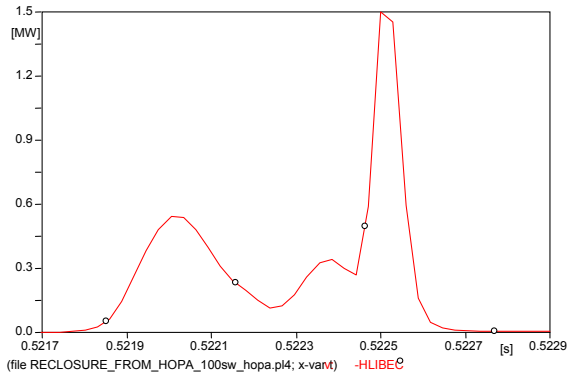

Figure 4.22 Power characteristic of surge arrester at Hopa when an arrester is used at Hopa (of Phase C)

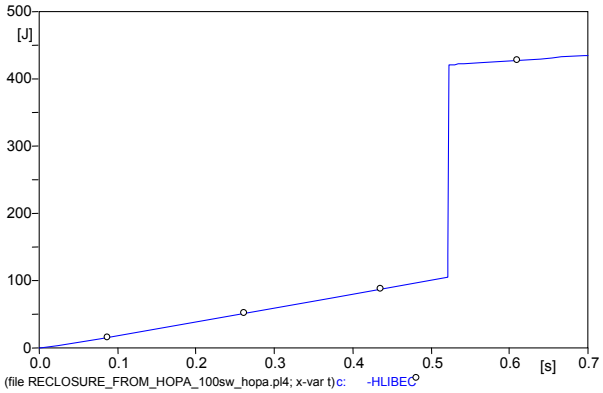

Figure 4.23 Energy absorption characteristic of surge arrester at Hopa when an arrester is used at Hopa (of Phase C)

Table 4.4 Overvoltages when the system is energized from Enguri and re-energized from Hopa (arrester is used at Hopa)

Measurement point	Mean values in pu	Mean values kV	Max values in pu	Max values kV
Hopa phase A	1.409 pu	253.62 kV	1.70 pu	306 kV
Hopa phase B	1.39 pu	250 kV	1.75 pu	315 kV
Hopa phase C	1.76 pu	316.8 kV	2.1 pu	378 kV
Enguri phase A	1.78 pu	320 kV	2.35 pu	423 kV
Enguri phase B	1.69 pu	304 kV	2.3pu	414 kV
Enguri phase C	2.722 pu	489 kV	3.75 pu	675 kV
All over nodes	2.752 pu	495.36 kV	3.75 pu	675 kV

When surge arrester of to cases which re-energizations take place from Enguri and Hopa are compared it can be deduced that values of power and energy decrease from 136.5 MW to 1.5 MW.

4.3.4 Simulation with one arrester placed at Enguri and a comparison of characteristics when the system is re-energized from Hopa and re-energized from Enguri

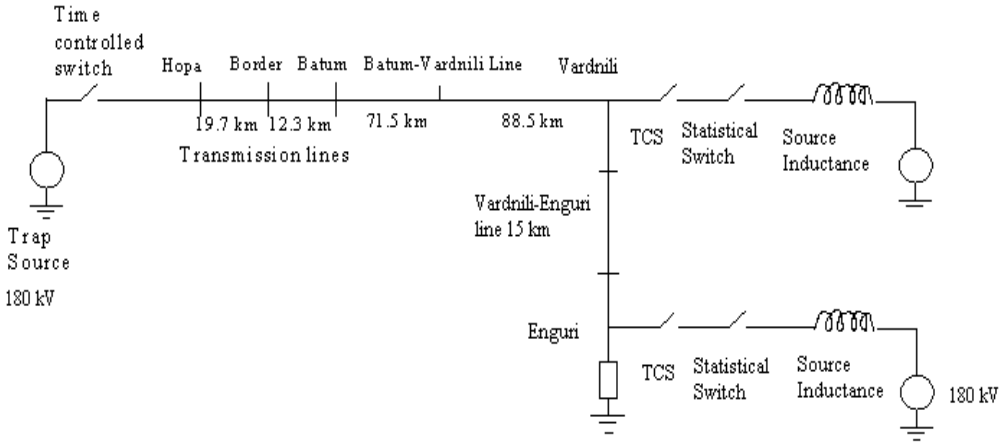

Figure 4.24 Location of the surge arrester installed at Enguri

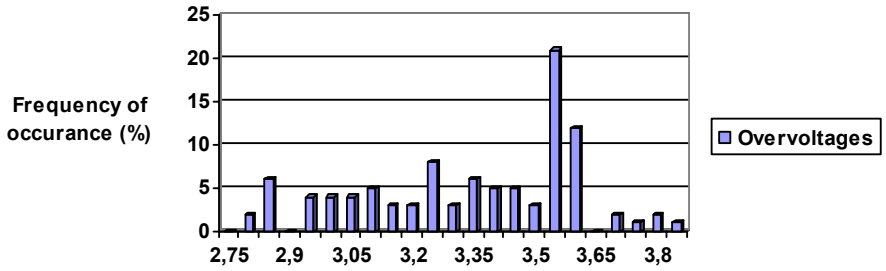

Figure 4.25 Histogram of voltage distribution for the maximum of the peaks of overall nodes when the system re-energized from Enguri and one arrester is used at Enguri

Distribution of overvoltages is severe when compared with the case where one arrester placed at Hopa whose placement is more useful in decreasing the

occurrence of overvoltages thus being at the receiving end of re-energization process.

The overvoltages at Hopa bus for the placement of surge arrester at Enguri reach 614 kV which is 3, 41 pu.

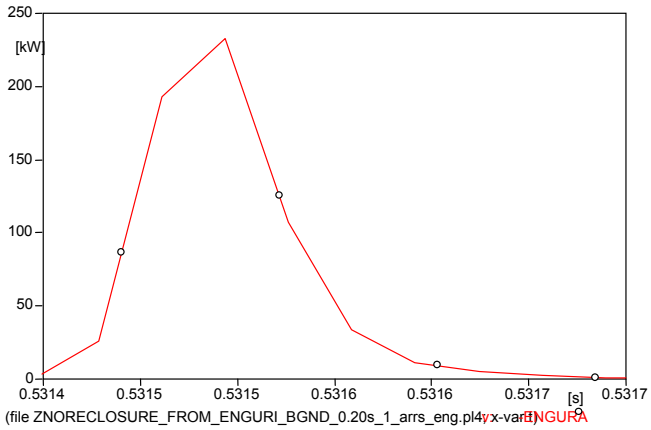

Figure 4.26 Power characteristic of surge arrester at Hopa when an arrester is used at Enguri (Phase A)

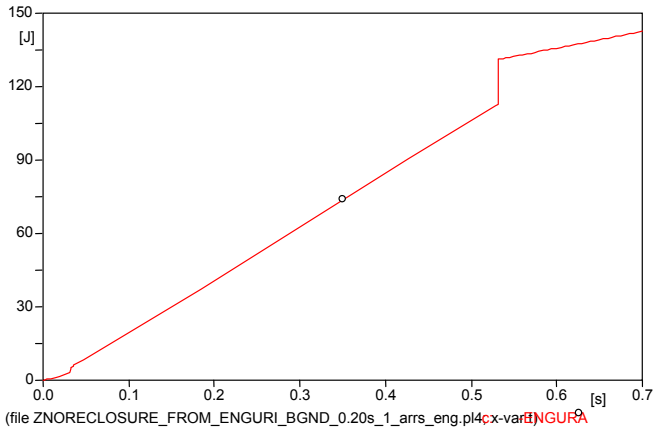

Figure 4.27 Energy absorption characteristic of surge arrester at Hopa when an arrester is used at Enguri

Table 4.5 Overvoltages when the system is energized from Hopa and re-energized from Enguri (arrester is used at Enguri)

Measurement point	Mean values in pu	Mean values kV	Max values in pu	Max values kV
Hopa phase A	1.399 pu	251.82 kV	1.70 pu	306 kV
Hopa phase B	1.314 pu	236.52 kV	1.65 pu	297 kV
Hopa phase C	1.762 pu	317.16 kV	2.2 pu	396 kV
Enguri phase A	1.7325 pu	311.85 kV	2.15 pu	387 kV
Enguri phase B	1.569 pu	282.42 kV	2 pu	360 kV
Enguri phase C	2.116 pu	380.88 kV	2.30 pu	414 kV
All over nodes	2.128 pu	383.04 kV	2.30 pu	414 kV

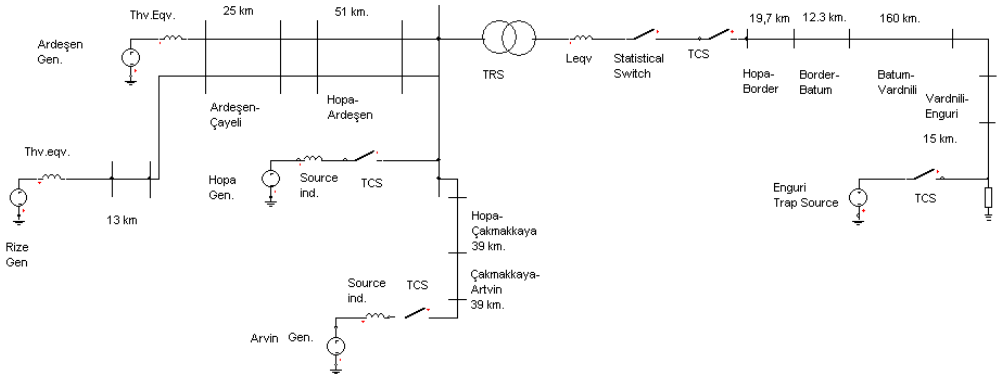

Figure 4.28 Network configuration of the system with surge arrester at Enguri re-energization from Hopa Bus

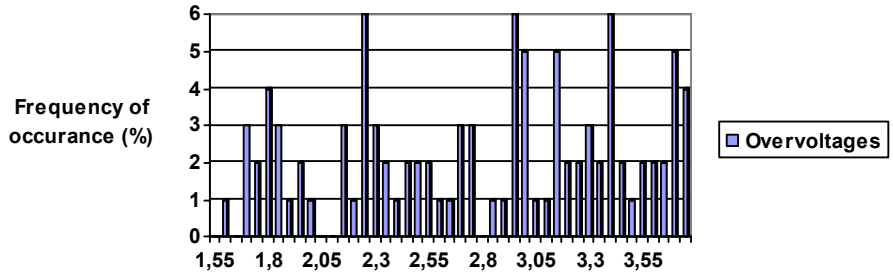

Figure 4.29 Histogram of voltage distribution for the maximum of the peaks of overall nodes when the system re-energized from Hopa and one arrester is used at Enguri

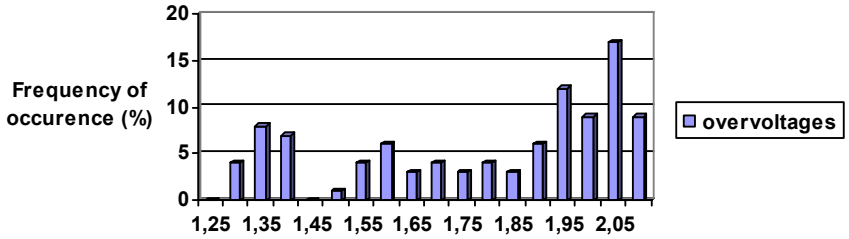

Figure 4.30 Histogram of voltage distribution for the maximum of the peaks at Hopa Bus when the system re-energized from Hopa and one arrester is used at Enguri

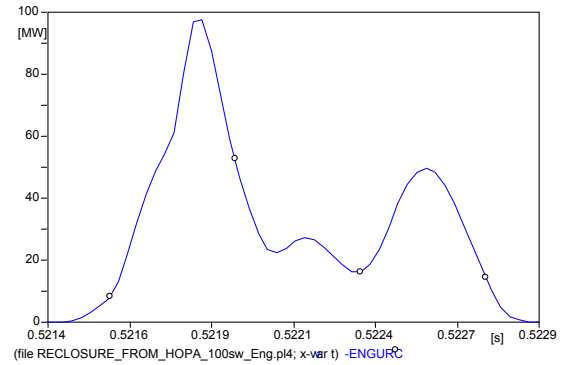

Figure 4.31 Power characteristic of surge arrester at Enguri

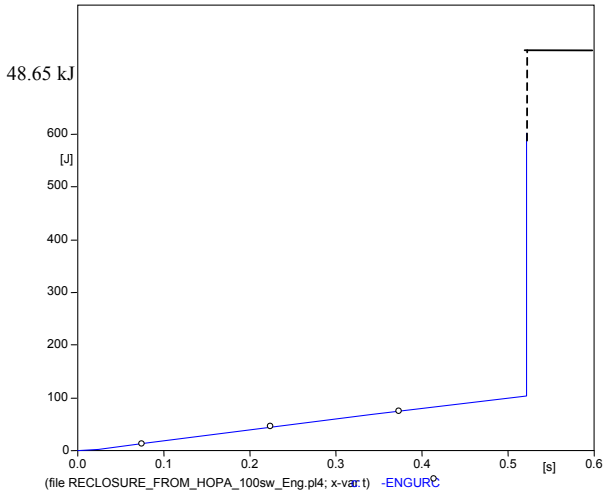

Figure 4.32 Energy characteristic of surge arrester at Enguri

When surge arrester characteristics of two different cases i.e. re-energization from Enguri and Hopa with one arresters at Enguri are compared it can be seen that due

to change in energization points, power characteristics differ from 240 kW to 98 MW and energy characteristics change from 175 J to 48.65 kJ.

Table 4.6 Overvoltages when the system is energized from Enguri and re-energized from Hopa (arrester is used at Enguri)

Measurement point	Mean values in pu	Mean values kV	Max values in pu	Max values kV
Hopa phase A	1.428 pu	257.04 kV	1.70 pu	306 kV
Hopa phase B	1.39 pu	250 kV	1.75 pu	315 kV
Hopa phase C	1.769 pu	318.42 kV	2.1 pu	378 kV
Enguri phase A	1.8305 pu	329 kV	2.3 pu	414 kV
Enguri phase B	1.711 pu	307.98 kV	2.25 pu	405 kV
Enguri phase C	2.75 pu	495 kV	3.75 pu	675 kV
All over nodes	2.7675 pu	498.15 kV	3.75 pu	675 kV

4.3.5 Simulation with one arrester placed in the midst of Vardnili-Batum line

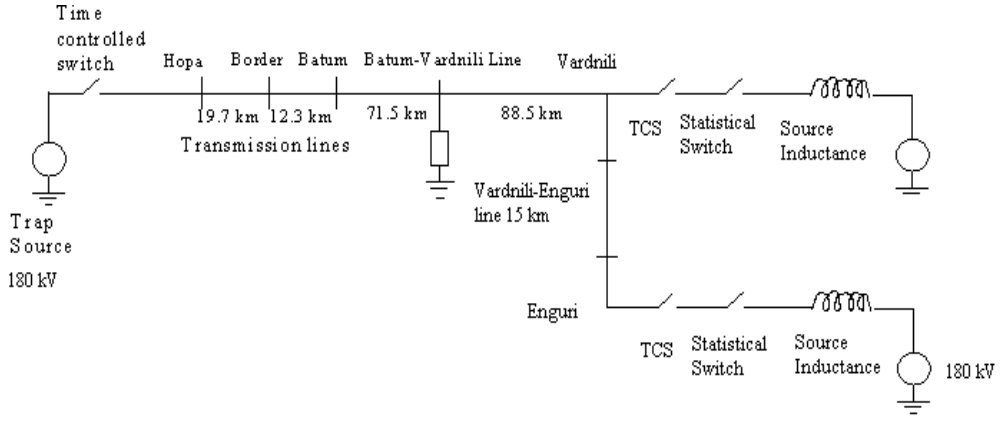

Figure 4.33 Location of the surge arrester installed at 71.5 km further than Batum

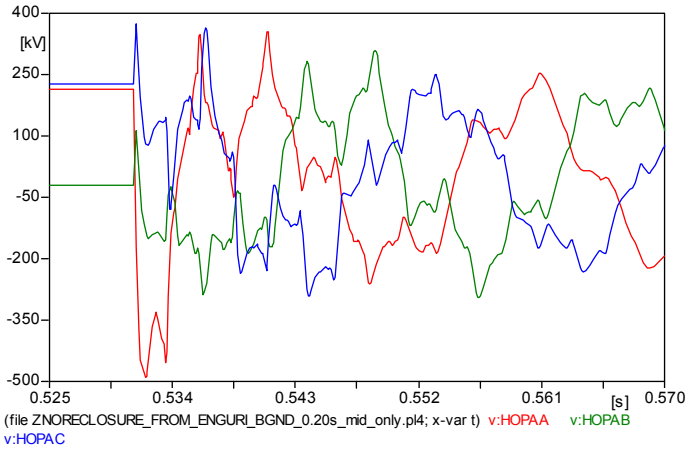

Figure 4.34 Receiving end voltage of line at Hopa when an arrester is used at 71.5 km further than Batum

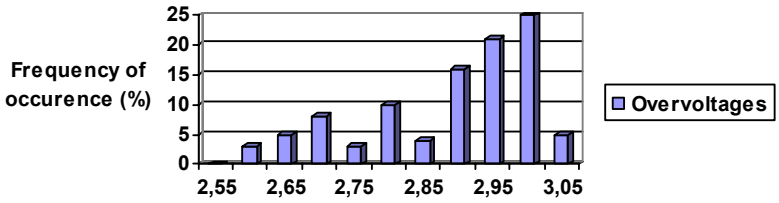

Figure 4.35 Histogram of voltage distribution for the maximum of the peaks at Hopa Bus phase A when the system re-energized from Hopa and one arrester is used at mid-point of Batum-Vardnili line

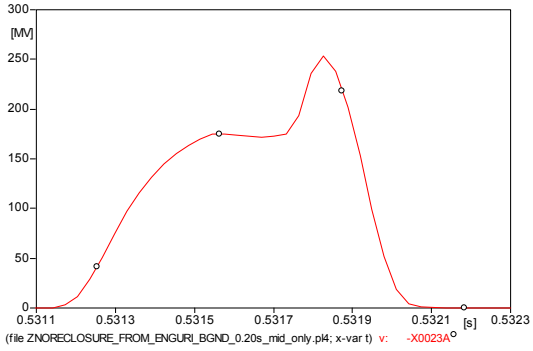

Figure 4.36 Power characteristic of surge arrester at Hopa when an arrester is used at 71.5 km further than Batum

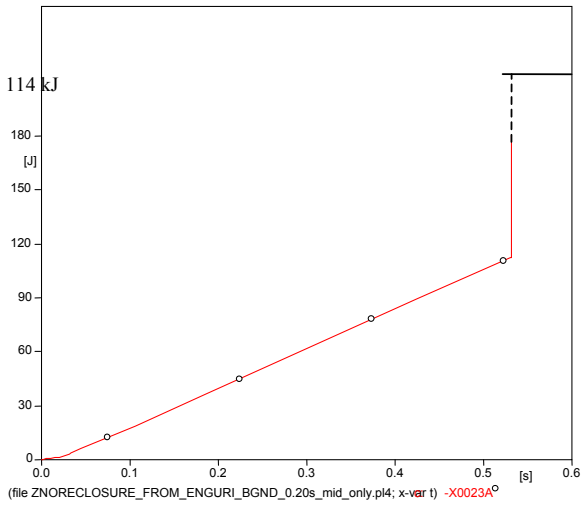

Figure 4.37 Energy absorption characteristic of surge arrester at Hopa when an arrester is used at 71.5 km further than Batum

Table 4.7 Overvoltages when the system is energized from Hopa and re-energized from Enguri (arrester is used at mid point of Batum-Vardnili line)

Measurement point	Mean values in pu	Mean values kV	Max values in pu	Max values kV
Hopa phase A	2.864 pu	515.52 kV	3.05 pu	549 kV
Hopa phase B	1.6930 pu	304.74 kV	2.10 pu	378 kV
Hopa phase C	2.1505 pu	378.07 kV	2.75 pu	495 kV
Mid point phase A	2.26 pu	406.8 kV	2.3 pu	414 kV
Mid point phase B	1.5205 pu	273.69 kV	1.90 pu	342 kV
Mid point phase C	1.7165 pu	308.97 kV	2.10 pu	378 kV

4.3.6 Simulation with two arresters placed in the midst of Vardnili-Batum line and Enguri

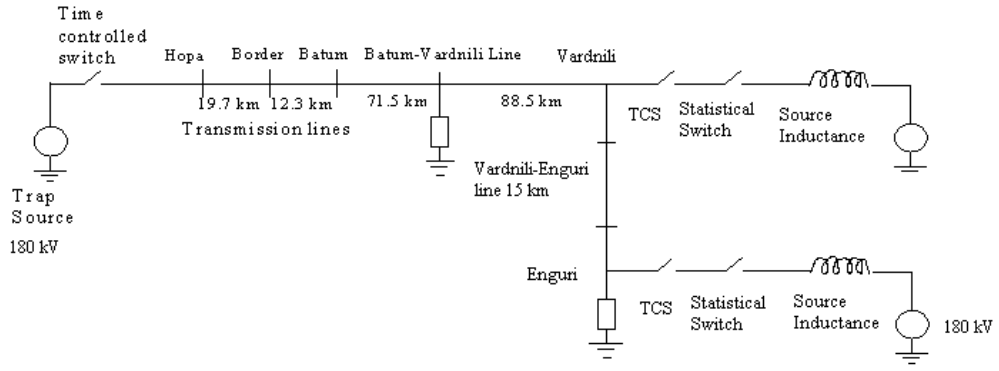

Figure 4.38 Arresters located at Enguri and at 71.5 km further than Batum

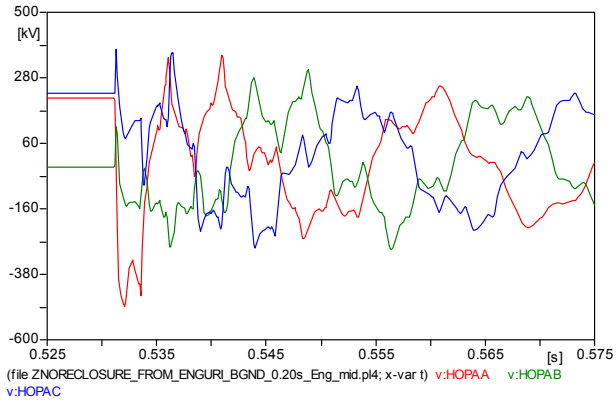

Figure 4.39 Voltage at Hopa open end when arresters are located at Enguri and at 71.5 km further than Batum

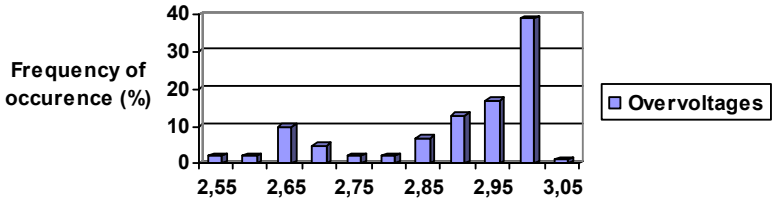

Figure 4.40 Histogram of overvoltage distribution at Hopa Bus (Phase A)

Power and energy characteristics of surge arrester at mid point of Vardnili when arresters are placed at Enguri and mid point of Vardnili

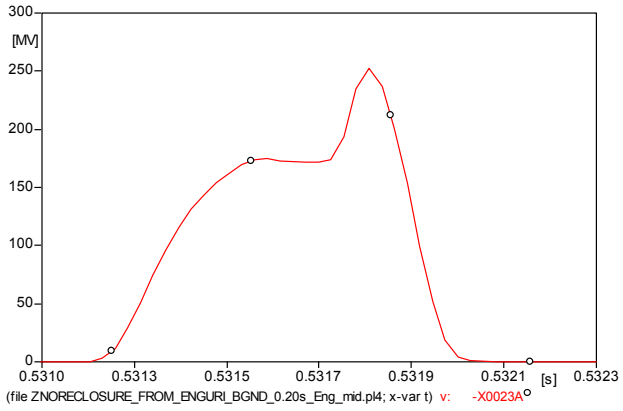

Figure 4.41 Power characteristic of surge arrester in the middle of Vardnili-Batum line when arresters are located at Enguri and at 71.5 km further than Batum

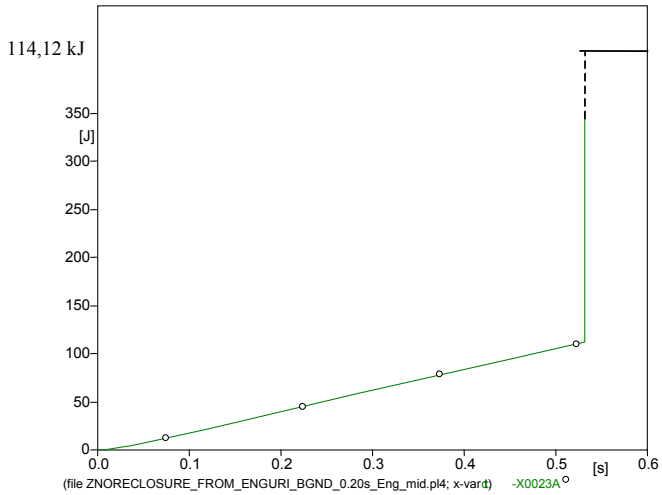

Figure 4.42 Energy characteristic of surge arrester in the middle of Vardnili-Batum line when arresters are located at Enguri and at 71.5 km further than Batum

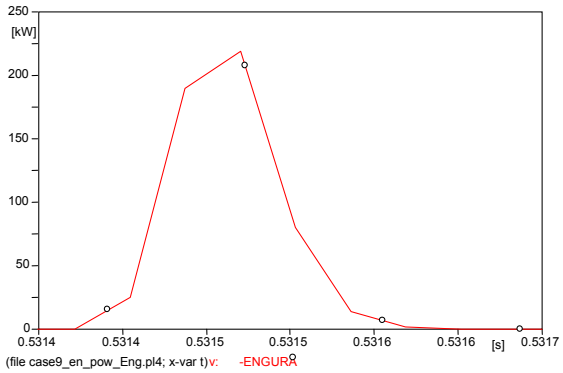

Figure 4.43 Power characteristic of surge arrester at Enguri when arresters are located at Enguri and at 71.5 km further than Batum

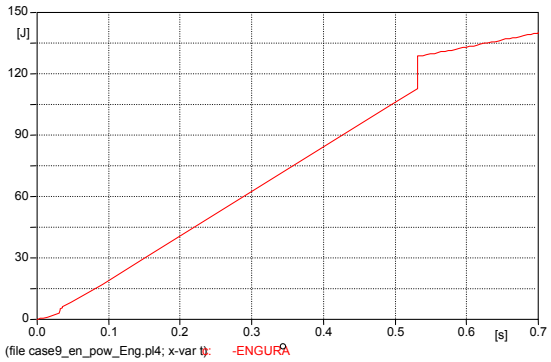

Figure 4.44 Energy characteristic of surge arrester at Enguri when arresters are located at Enguri and at 71.5 km further than Batum

Table 4.8 Overvoltages when the system is energized from Hopa and re-energized from Enguri (arresters are used at mid point of Batum-Vardnili line and Enguri)

Measurement point	Mean values in pu	Mean values kV	Max values in pu	Max values kV
Hopa phase A	2.8675 pu	516.15 kV	3.05 pu	549 kV
Hopa phase B	1.713 pu	308.34 kV	2.10 pu	378 kV
Hopa phase C	2.1665 pu	389.97 kV	2.6 pu	468 kV
Mid point phase A	2.2635 pu	407.43 kV	2.3 pu	414 kV
Mid point phase B	1.5265 pu	274.77 kV	1.90 pu	342 kV
Mid point phase C	1.73 pu	311.4 kV	2.15 pu	387 kV
Enguri phase A	1.71 pu	307.8 kV	1.9 pu	342 kV

4.3.7 Simulation with two arresters placed in the midst of Vardnili-Batum line and Hopa

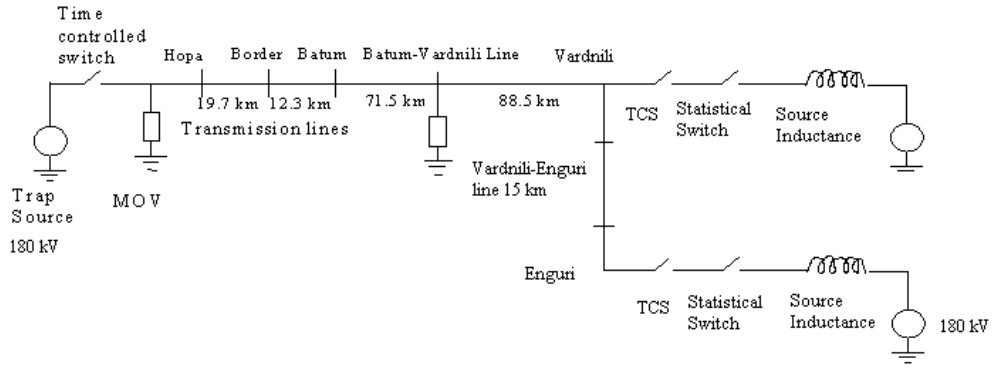

Figure 4.45 Arresters located at Hopa and at 71.5 km further than Batum

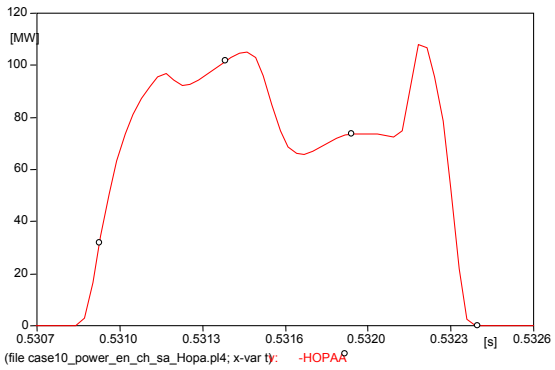

Figure 4.46 Power characteristic at Hopa when arresters are located at Hopa and at 71.5 km further than Batum

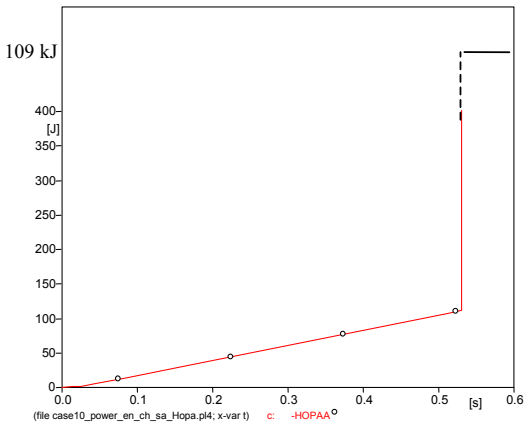

Figure 4.47 Energy characteristic of surge arrester at Hopa

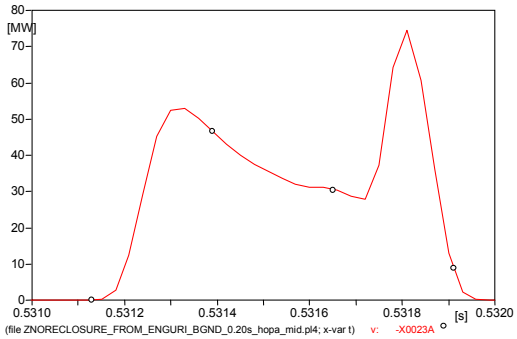

Figure 4.48 Power characteristic of surge arrester at mid point when arresters are placed at Hopa and mid point of Vardnili

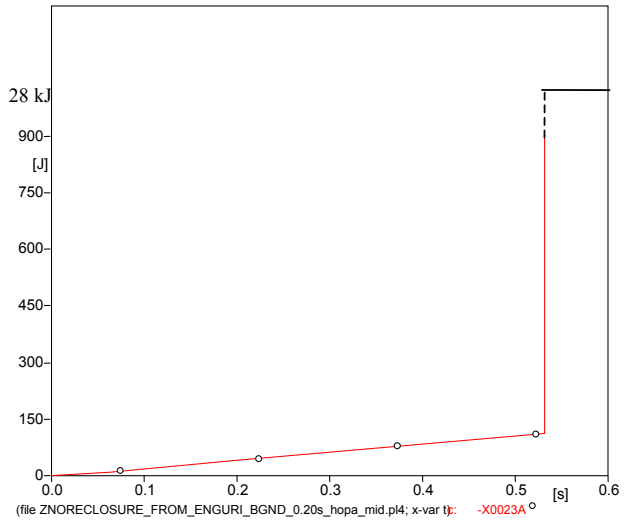

Figure 4.49 Energy characteristic of surge arrester at mid point when arresters are placed at Hopa and mid point of Vardnili

Table 4.9 Overvoltages when the system is re-energized from Enguri (arresters are used at mid point of Batum-Vardnili line and Hopa)

Measurement point	Mean values in pu	Mean values kV	Max values in pu	Max values kV
Hopa phase A	2.18 pu	392,4 kV	2,25 pu	405 kV
Hopa phase B	1.6195 pu	291,51 kV	2.0 pu	360 kV
Hopa phase C	1,9985 pu	359,73 kV	2.15 pu	387 kV
Mid point phase A	2,1565 pu	388,17 kV	2.2 pu	396 kV
Mid point phase B	1.456 pu	262 kV	1.90 pu	342 kV
Mid point phase C	1.646 pu	296,28 kV	2.05 pu	369 kV
Enguri phase A	1.7005 pu	306.09 kV	1.9 pu	342 kV

4.3.8 Simulation with two arresters placed at Enguri and Hopa

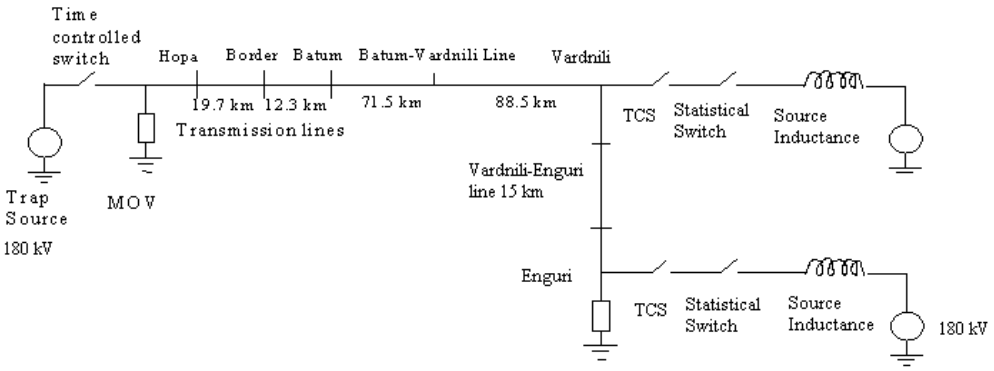

Figure 4.50 Arresters located at Hopa and at Enguri

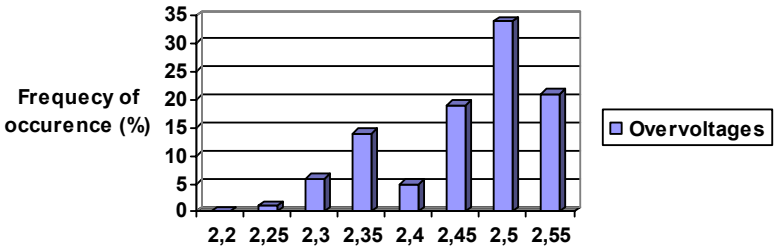

Figure 4.51 Histogram of overvoltage distribution at all output nodes

Power and energy characteristics of surge arrester located at Enguri in case of there exists two arresters; one at Hopa and the other at Enguri

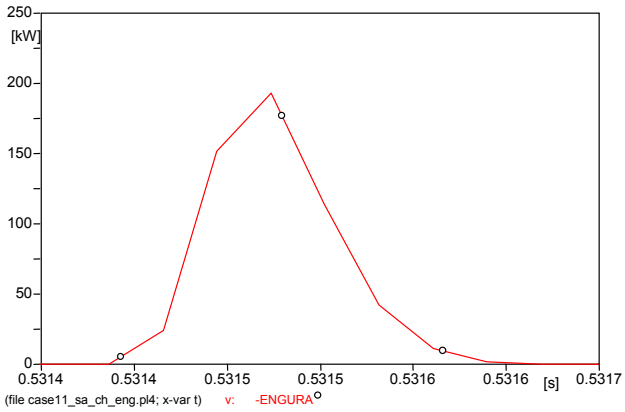

Figure 4.52 Power characteristics of surge arrester located at Enguri when arresters are placed at Hopa and at Enguri

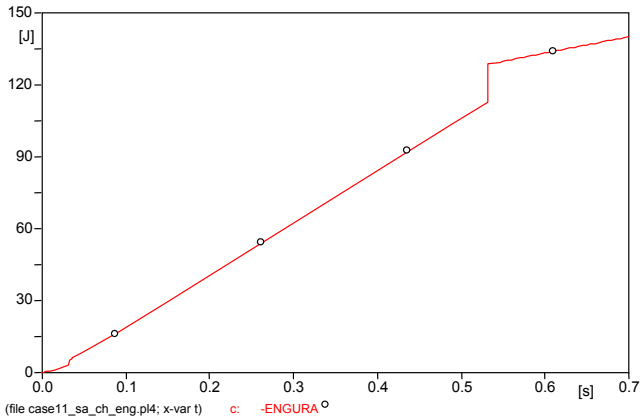

Figure 4.53 Energy characteristics of surge arrester located at Enguri when arresters are placed at Hopa and at Enguri

Power and energy characteristics of surge arrester located at Hopa in case of there exists two arresters; one at Hopa and the other at Enguri

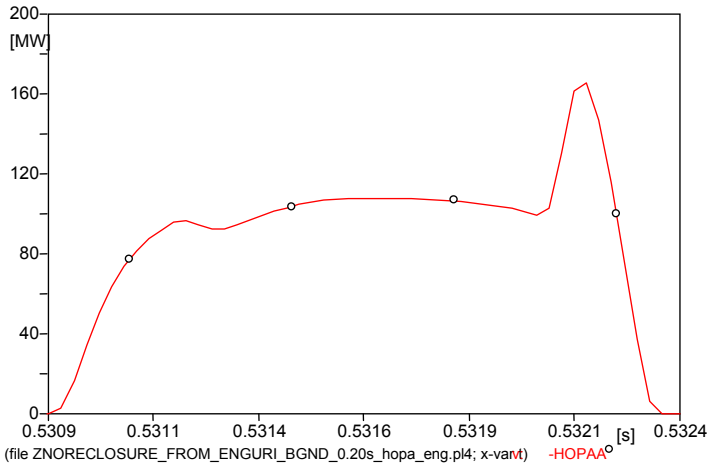

Figure 4.54 Power characteristics of surge arrester located at Enguri when arresters are placed at Hopa and at Enguri

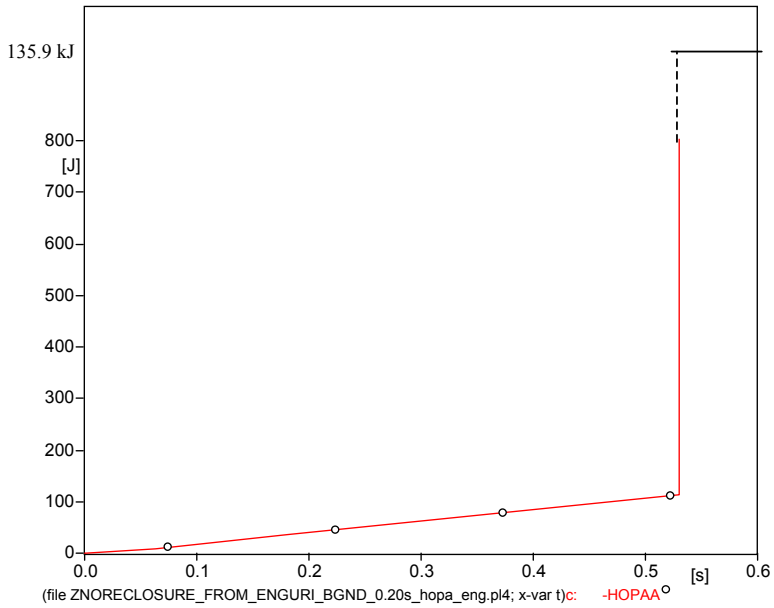

Figure 4.55 Energy characteristics of surge arrester located at Enguri when arresters are placed at Hopa and at Enguri

Table 4.10 Overvoltages when the system is energized from Hopa and re-energized from Enguri (arresters are used at Hopa and Enguri busses)

Measurement point	Mean values in pu	Mean values kV	Max values in pu	Max values kV
Hopa phase A	2.2225 pu	400.05 kV	2.3 pu	414 kV
Hopa phase B	1.5885 pu	285,93 kV	2.0 pu	360 kV
Hopa phase C	2.0275 pu	364.95 kV	2.2 pu	396 kV
Mid point phase A	2.399 pu	431.82 kV	2.55 pu	459 kV
Mid point phase B	1.4655 pu	263.79 kV	2.20 pu	396 kV
Mid point phase C	1.6565 pu	298.17 kV	2.15 pu	387 kV
Enguri phase A	1.7285 pu	311.13 kV	1.85 pu	333 kV
All output nodes	2.4355 pu	438.39 kV	2.55 pu	459 kV

4.3.9 Simulation with two arresters placed at Enguri and Hopa when the line is re-energized from Hopa

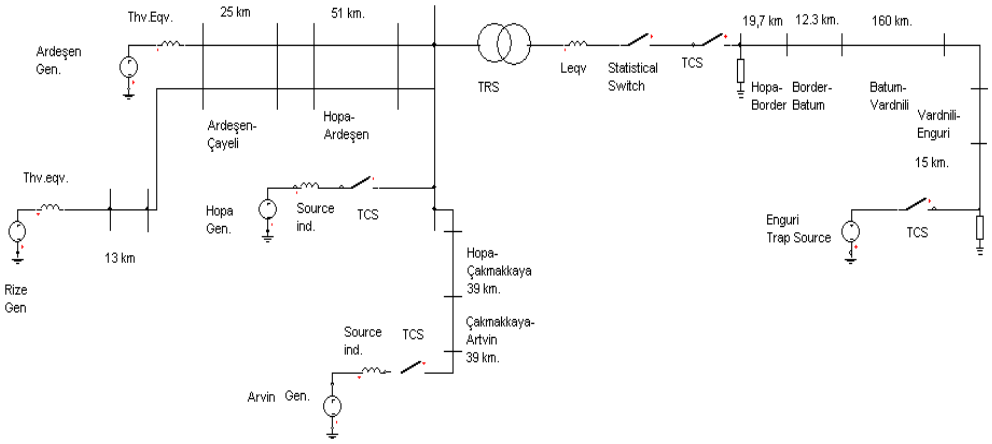

Figure 4.56 Location of the surge arrester installed at Hopa and Enguri

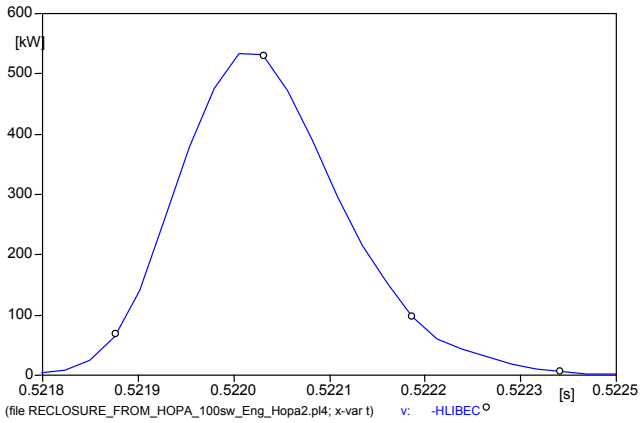

Figure 4.57 Power characteristics of the surge arrester placed at Hopa

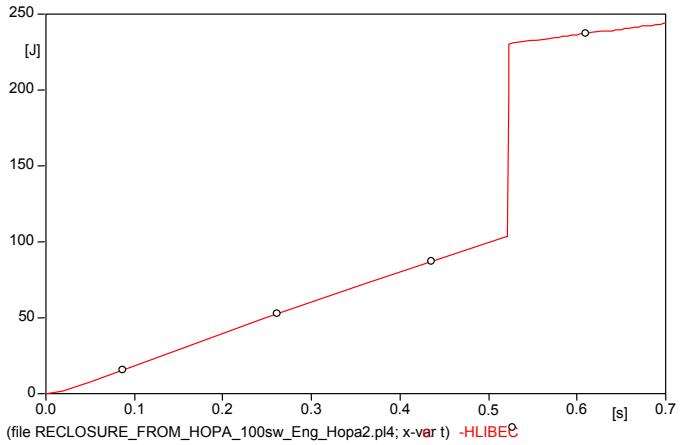

Figure 4.58 Energy characteristics of the surge arrester placed at Hopa

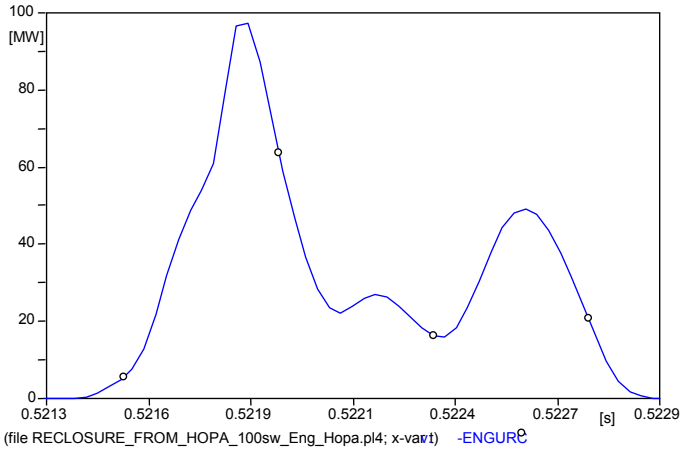

Figure 4.59 Power characteristics of the surge arrester placed at Enguri

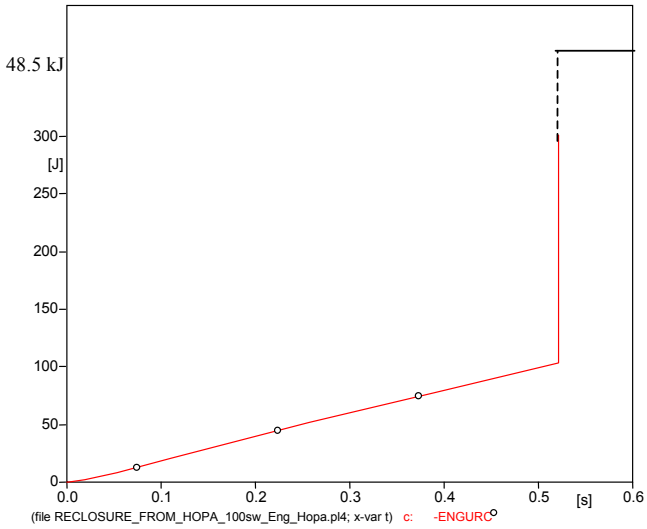

Figure 4.60 Energy characteristics of the surge arrester placed at Enguri

Table 4.11 Overvoltages when arresters are placed at Hopa and Enguri

Measurement point	Mean values in pu	Mean values kV	Max values in pu	Max values kV
Hopa phase A	1.3555 pu	243.99 kV	1.70 pu	306 kV
Hopa phase B	1.3105 pu	297 kV	1,65 pu	297 kV
Hopa phase C	1.7415 pu	313.47 kV	2.1 pu	378 kV
Enguri phase A	1.672 pu	300.99 kV	2.15 pu	387 kV
Enguri phase B	1.5705 pu	282.69 kV	2 pu	360 kV
Enguri phase C	2.109 pu	379.62 kV	2.30 pu	414 kV
All output nodes	2.119 pu	381.42 kV	2.30 pu	414 kV

4.3.10 Simulation with three arresters placed at Enguri, Hopa and at the 71,5th km of Batum-Vardnili line

The following graphic belongs to a configuration at which 3 arresters are used to reduce the surges. One in the beginning of the line at Hopa, one after 103.5 km. and the last one is placed at the end of the line, Enguri, which is 103.5 km further.

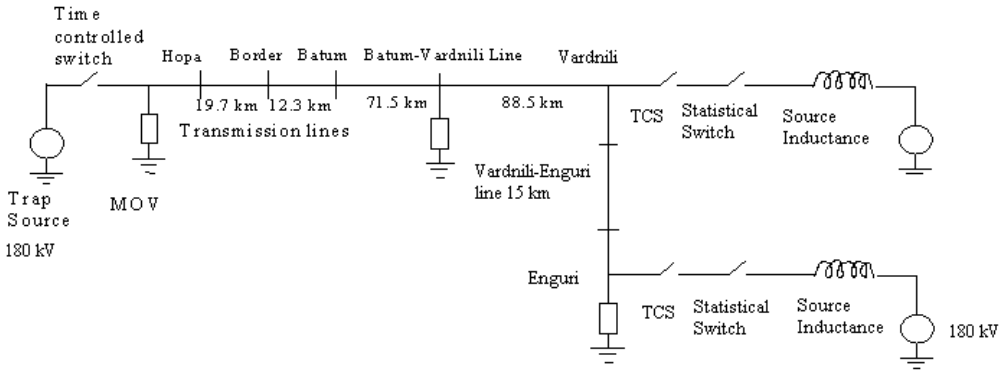

Figure 4.61 Transmission line configuration (with 3 arresters)

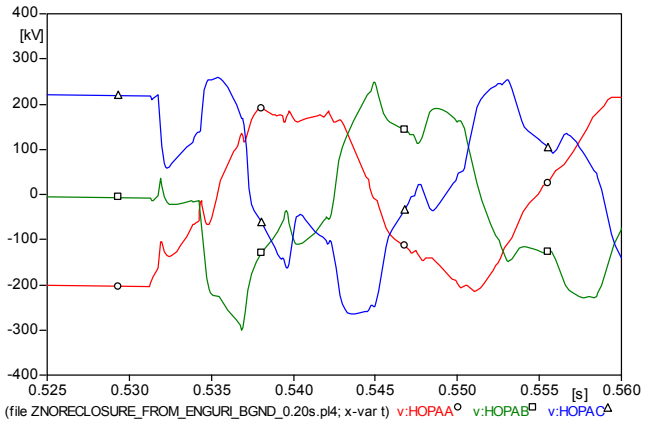

Figure 4.62 Receiving end voltage of line at Hopa when 3 arresters are used

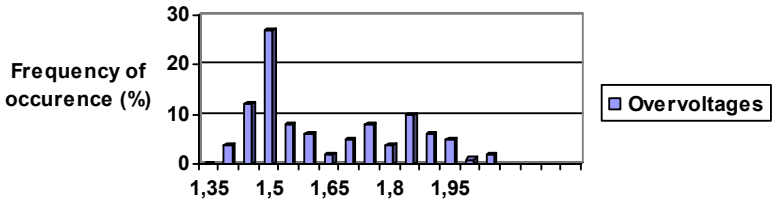

Figure 4.63 Histogram of overvoltage distribution at Hopa Bus (Phase C)

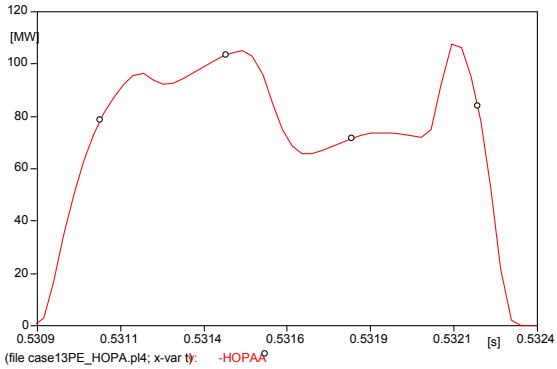

Figure 4.64 Power characteristic of surge arrester at Hopa

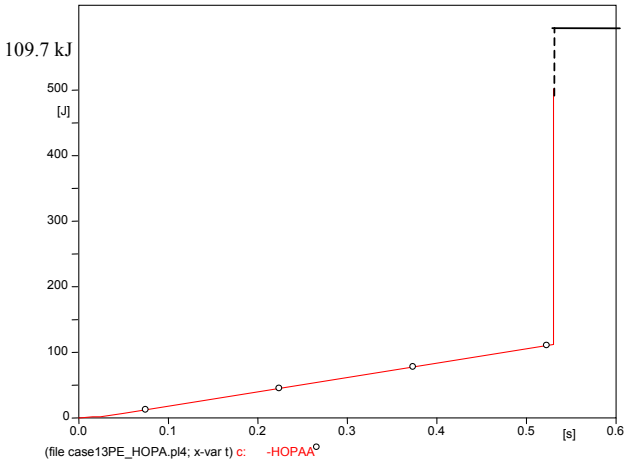

Figure 4.65 Energy characteristic of surge arrester at Hopa

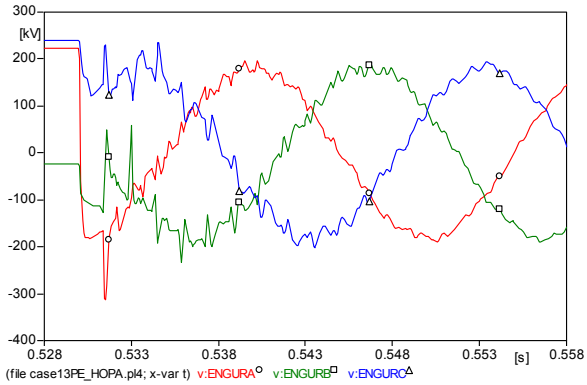

Figure 4.66 Voltage characteristics at Enguri bus

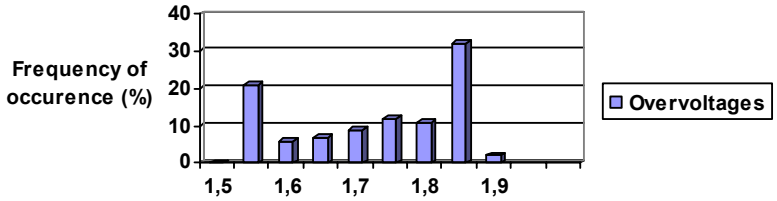

Figure 4.67 Histogram of overvoltage distribution at Enguri Bus (Phase A)

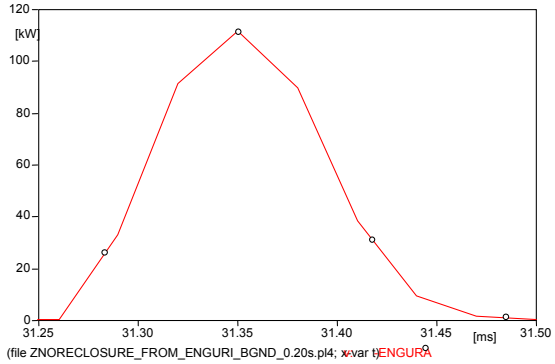

Figure 4.68 Power characteristic of surge arrester at Enguri

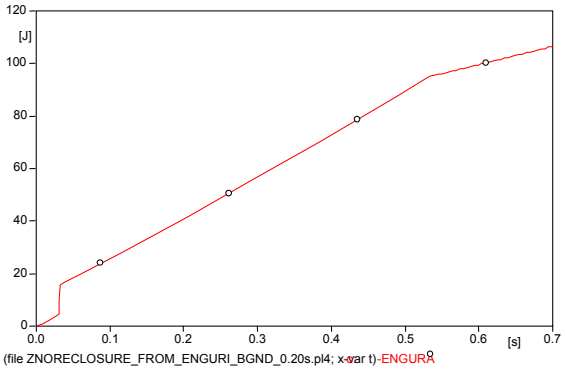

Figure 4.69 Energy characteristic of surge arrester at Enguri

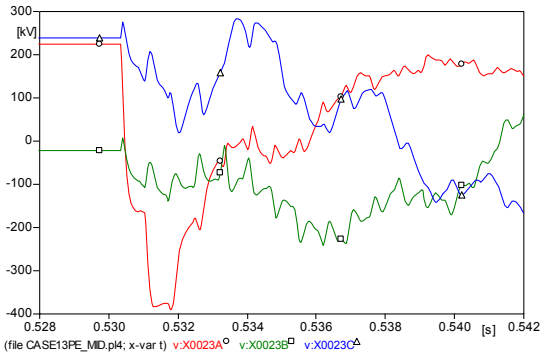

Figure 4.70 Voltage characteristics at mid point of Vardnili-Batum line

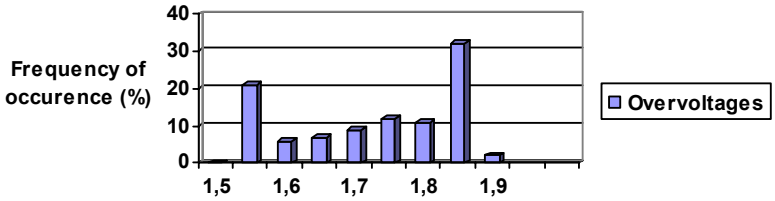

Figure 4.71 Voltage distribution at Enguri (Phase A)

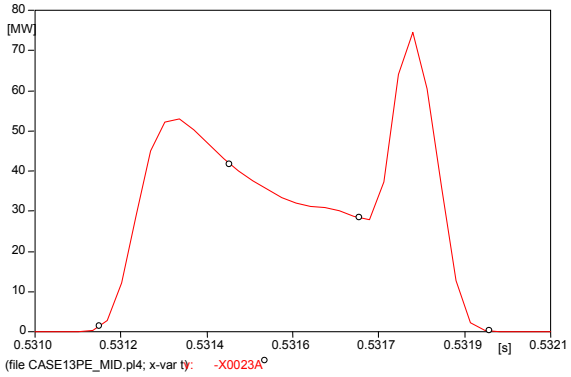

Figure 4.72 Power characteristic of surge arrester at mid point

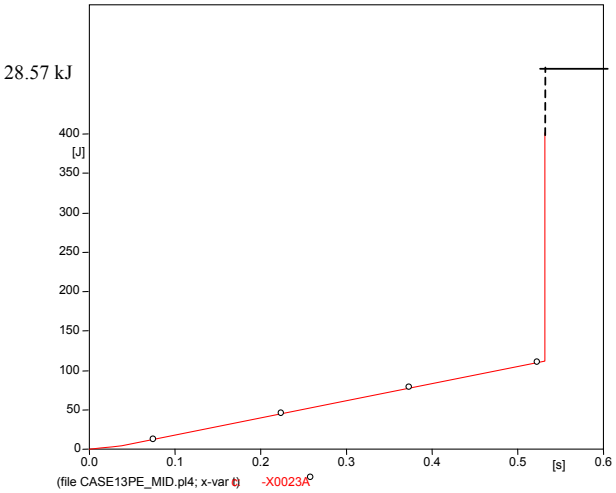

Figure 4.73 Energy characteristic of surge arrester at mid point

Table 4.12 Overvoltages when the system is re-energized from Hopa (arresters are placed at Hopa, Enguri and mid point of Vardnili-Batum line)

Measurement point	Mean values in pu	Mean values kV	Max values in pu	Max values kV
Hopa phase A	1.636 pu	294.48 kV	1.90 pu	342 kV
Hopa phase B	1.7245 pu	310.41 kV	2 pu	360 kV
Hopa phase C	1.6175 pu	291.15 kV	2.05 pu	369 kV
Mid point phase A	1.442 pu	259.56 kV	1.75 pu	315 kV
Mid point phase B	1.625 pu	292.5 kV	1.95 pu	351 kV
Mid point phase C	1.73 pu	311.4 kV	2.15 pu	387 kV
Enguri phase A	1.703 pu	306.54 kV	1.9 pu	342 kV
All nodes	1.821 pu	327.78 kV	2.05 pu	342 kV

4.4 SIMULATION RESULTS

The simulation results of surge arrester application against switching surges are illustrated in this section. The role of these surge arresters is to prevent energization and re-energization overvoltage surges, occurring on the HV overhead lines. The general practice is to install surge arresters at appropriate location/locations considering economical criteria.

The effect of installation of surge arresters for surge magnitudes at different parts is presented in figures. Due to energization and re-energization points overvoltages at buses vary. The distributions of peak overvoltages among all output nodes and at important nodes are presented after each case to make a comparison possible between basic cases and variations.

CHAPTER 5

CONCLUSION

5.1 INTRODUCTION

This final chapter summarises the research carried out and its implications. The research was carried out in the area of overvoltage protection of transmission line systems and particularly focused on investigating overvoltage conditions experienced from energization activity as well as from re-energization processes.

The studies are carried out through computer simulations, using ATPDraw which is a graphical, mouse-driven preprocessor to the Alternative Transient Program (ATP) version of Electro-Magnetic Transient Program (EMTP) on the MS-Windows platform. In ATPDraw an electric circuit can be constructed by using the mouse and selecting components from menus, and then ATPDraw generates the ATP input file. ATP is a general-purpose computer program for simulating high-speed transient effects in electrical power systems. [3]

5.2 COMPARISON OF ENERGIZATION VERSUS RE-ENERGIZATION

Re-energization results in very high overvoltages which will require high insulation levels. Therefore these overvoltages must be reduced; especially the ones generated in re-energization transients are quite high and certainly can not be tolerated in a practical line design. Since they will give rise to insulation failures.

One of the means in reducing these is utilization of resistors in energization. But due to problems faced, which are not operating on time, thermal incapability and as a result heating and breakdown, other means were to be investigated.

The new technology is to use ZnO arresters which have different characteristics from the SiO arresters. The problem is that of energy dissipation of arresters which is very high in the case of switching surges. New arresters having this energy dissipation capability are available.

Investigated topics are where to put them and energy dissipation capacities where 3 arresters are used to divide it, at first one by one and in sets of utilization two of them and in the end 3 of them were used together.

It can be seen from the work carried out that ZnO arresters placed at suitable locations on the transmission lines will be very effective in the reduction of switching surges. And therefore economic insulation levels can be used on these systems.

REFERENCES

[1] Hussain Shareef, "Overvoltage protection of low voltage systems", Ms Thesis submitted to METU, December 2002

[2] O.Bülent Tör, "Switching overvoltages on the new interconnection between Turkey and Bulgaria", Ms Thesis submitted to METU, September 2001

[3] ATP-DRAW MANUAL, October 2002

[4] Nevzat Özay, "Analysis of energisation transients of transmission lines", Ph.D. Thesis submitted to the Victoria University of Manchester, September 1971

[5] J.R. Riberio, M.E.McCallum "An Application of Metal Oxide Surge Arresters in the elimination of need for closing resistors in EHV breakers" IEEE Transactions on Power Delivery, Vol.4, No.1, pp 282-291, January 1989

[6] ATP RULE BOOK, European EMTP-ATP Users Group e.V,1999.

[7] Jonathan J.Woodworth, Herman E.Fletcher, "New surge arrester technology offers substantial improvement in protection and reliability", Cooper Power systems, May 1990

[8] Jonathan J.Woodworth , "Overvoltage surge protection of the 90's", Cooper Power Systems, March 1991

[9] R. Willheim, M. Waters, Neutral Grounding in High Voltage Transmission, Elsevier Publishing Company, 1956 pp 71-76

[10] ABB Buyers Guide Edition 3, 2003

[11] ABB Power Technology Products, Technical Information, 2001-08